

000 001 002 003 004 005 006 007 008 009 010 011 012 013 014 015 016 017 018 019 020 021 022 023 024 025 026 027 028 029 030 031 032 033 034 035 036 037 038 039 040 041 042 043 044 045 046 047 048 049 050 051 052 053 BA-LoRA: BIAS-ALLEVIATING LOW-RANK ADAPTA- TION TO MITIGATE CATASTROPHIC INHERITANCE IN LARGE LANGUAGE MODELS

006 **Anonymous authors**

007 Paper under double-blind review

ABSTRACT

Parameter-efficient fine-tuning (PEFT) has become a de facto standard for adapting Large Language Models (LLMs). However, we identify a critical vulnerability within popular low-rank adaptation methods like LoRA: **they can exacerbate** "Catastrophic Inheritance"—the unchecked propagation of biases, noise, and data imbalances from pre-training. This phenomenon can degrade model robustness and fairness, undermining the benefits of efficient adaptation. To address this, we introduce Bias-Alleviating Low-Rank Adaptation (BA-LoRA). Our approach is founded on a principled decomposition of Catastrophic Inheritance into three core challenges: Knowledge Drift, Representation Collapse, and Overfitting to Noise. BA-LoRA systematically mitigates these issues by incorporating a trio of targeted regularizers—consistency, diversity, and SVD—designed to preserve core knowledge, enforce representational richness, and promote robust, low-rank output representations. We conduct comprehensive evaluations on a suite of natural language understanding (NLU) and generation (NLG) tasks using diverse, prominent open-source language models (e.g., LLaMA-2-7B and DeBERTa-v3-base). Our results show that BA-LoRA not only outperforms state-of-the-art LoRA variants in terms of performance and stability, but also demonstrates quantitatively superior robustness and bias mitigation on targeted evaluations. This confirms its ability to counteract the adverse effects of Catastrophic Inheritance.

1 INTRODUCTION

Large language models (LLMs) like GPT-4 (OpenAI, 2023) and LLaMA (Touvron et al., 2023) have redefined the state-of-the-art in natural language processing (NLP), largely due to their training on vast, web-scale corpora (Zhao et al., 2023; Chang et al., 2024). This strategy, while enabling unprecedented generalization (Gao et al., 2020; Penedo et al., 2023), comes at a cost: models inevitably inherit and internalize the biases, noise, and imbalances latent within these unfiltered datasets (Parashar et al., 2024; Liu & He, 2024; Chen et al., 2024b).

Recent research confirms that these inherited flaws can degrade model performance and persist even after fine-tuning, posing significant risks to fairness and safety (Qi et al., 2023; Bommasani et al., 2021; Mallen et al., 2022; Carlini et al., 2023). For example, noise within the training data can degrade model generalization (Chen et al., 2024a), while the long-tailed distribution of concepts can cause LLMs to overemphasize overrepresented topics (Zhu et al., 2024; Dong et al., 2023).

This phenomenon, termed "Catastrophic Inheritance" (Chen et al., 2024a), arises when models inherit such biases, noise, and imbalances from pre-training; **we focus on how these inherited artifacts can be further amplified during downstream fine-tuning**, and this has spurred investigations into mitigation strategies. While constructing less biased datasets and developing more robust model architectures are prominent approaches (Liu & He, 2024), this study explores an alternative: innovations in fine-tuning. Fine-tuning is a powerful method for enhancing task-specific performance and aligning models with user intent (Han et al., 2024; Ouyang et al., 2022). However, its computational demands are substantial; for instance, 16-bit fine-tuning of a Llama-65B model requires over 780 GB of GPU memory (Dettmers et al., 2024). To address these limitations, parameter-efficient fine-tuning (PEFT) techniques, such as Low-Rank Adaptation (LoRA) (Hu et al., 2021), have gained prominence.

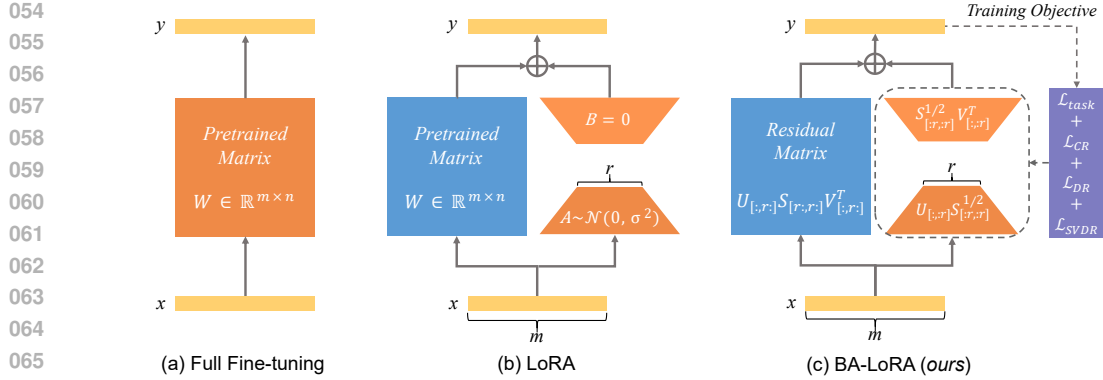


Figure 1: Comparison of three fine-tuning frameworks: (a) Full Fine-tuning, updating the entire matrix W ; (b) LoRA, training a low-rank adapter for a frozen W ; and (c) our proposed BA-LoRA. Blue and orange modules denote frozen and trainable parameters, respectively. Our method first initializes its adapter and residual matrix (W^{res}) from the SVD of W (PiSSA-style). It then augments the task loss ($\mathcal{L}_{\text{task}}$) with three regularization terms (purple module) designed to mitigate catastrophic inheritance by preserving knowledge, promoting diversity, and focusing on core data patterns.

LoRA enables efficient fine-tuning by approximating parameter updates using low-rank matrices. As illustrated in Figure 1 (a), Full Fine-tuning directly updates the entire weight matrix W . In contrast, LoRA (Figure 1 (b)) introduces a learnable low-rank adapter $\Delta W = AB$, where $A \in \mathbb{R}^{m \times r}$ and $B \in \mathbb{R}^{r \times n}$ are trainable matrices with a rank $r \ll \min(m, n)$. Only A and B are updated, while the original weights W remain frozen. By initializing A with scaled random values and B to zero, LoRA ensures the adapter has no effect at the start of training. The forward pass is then computed as $Y = X(W + AB)$, significantly reducing computational costs (Hu et al., 2021).

While PEFT methods like LoRA offer remarkable efficiency, their constrained, low-rank updates introduce a critical vulnerability: they **can exacerbate Catastrophic Inheritance when fine-tuning on noisy or imbalanced data without explicit regularization**. By forcing all model adjustments through a low-dimensional bottleneck, these methods may lack the capacity to correct for inherited biases, instead amplifying spurious correlations from pre-training data. To bridge this gap, we argue that a more principled approach is needed. We first deconstruct Catastrophic Inheritance into three primary failure modes: **Knowledge Drift**, where the model **unintentionally** forgets robust pre-trained knowledge while learning new tasks (Kirkpatrick et al., 2017); **Representation Collapse**, where fine-tuning on imbalanced data causes output diversity to plummet (Bardes et al., 2021); and **Overfitting to Noise**, where the model learns spurious correlations from the training data that hinder generalization (Chen et al., 2019). This paper introduces Bias-Alleviating Low-Rank Adaptation (BA-LoRA), a novel method that systematically mitigates these issues. As depicted in Figure 1 (c), BA-LoRA builds upon the efficient PiSSA (Meng et al., 2024) initialization and incorporates a trio of regularizers: a consistency regularizer to combat Knowledge Drift, a diversity regularizer to prevent Representation Collapse, and an SVD regularizer to mitigate Overfitting to Noise. Recognizing the differences between NLU and NLG tasks, we tailor these strategies accordingly.

Our comprehensive evaluation establishes BA-LoRA’s superior performance and deconstructs the sources of its effectiveness. BA-LoRA consistently outperforms leading LoRA variants across diverse benchmarks, including mathematical reasoning, coding, and conversational AI for NLG, as well as the GLUE benchmark (Wang et al., 2018) for NLU, using models such as LLaMA-2-7B (Touvron et al., 2023) and DeBERTa-v3-base (He et al., 2021). Crucially, we move beyond standard leaderboards to test our central hypothesis. **An empirical comparison on models pre-trained with clean (RoBERTa (Liu et al., 2019)) versus noisier web-scale (T5 (Raffel et al., 2020)) data shows that BA-LoRA achieves larger gains on the latter, which is consistent with our hypothesis that BA-LoRA is particularly beneficial when mitigating the effects of inherited noise.** This primary finding is supported by comprehensive ablation studies and qualitative visualizations that confirm the necessity of our three-pronged strategy. Together, these results not only demonstrate BA-LoRA’s superiority but also validate our theoretical framework for understanding and mitigating this phenomenon.

108

2 METHOD

109

2.1 PRINCIPAL SINGULAR VALUES AND SINGULAR VECTORS ADAPTATION (PiSSA)

110 As a variant of LoRA, PiSSA accelerates convergence by retaining the core LoRA architecture but
 111 changing the initialization. It leverages the principal components of the original weight matrix W to
 112 initialize the adapter matrices A and B , and stores the remaining components in a residual matrix
 113 $W^{\text{res}} \in \mathbb{R}^{m \times n}$. We write the SVD of $W \in \mathbb{R}^{m \times n}$ as $W = USV^T$, where U and V contain the
 114 left and right singular vectors and S is a diagonal matrix of singular values sorted in descending
 115 order. PiSSA partitions the singular components into principal $\{U_{[:,r]}, S_{[r,:r]}, V_{[:,r]}\}$ and residual
 116 $\{U_{[:,r]}, S_{[r,:r]}, V_{[:,r]}\}$ parts, where r is the user-specified adapter rank. The principal components
 117 are then used to initialize the low-rank adapter with $A \in \mathbb{R}^{m \times r}$ and $B \in \mathbb{R}^{r \times n}$.
 118

$$119 \quad A = U_{[:,r]} S_{[r,:r]}^{1/2} \in \mathbb{R}^{m \times r} \quad (1)$$

$$120 \quad B = S_{[r,:r]}^{1/2} V_{[:,r]}^T \in \mathbb{R}^{r \times n} \quad (2)$$

121 The residual matrix W^{res} remains frozen during fine-tuning:
 122

$$123 \quad W^{\text{res}} = U_{[:,r]} S_{[r,:r]} V_{[:,r]}^T \in \mathbb{R}^{m \times n} \quad (3)$$

124 PiSSA preserves the pre-trained model’s full capacity at the start of fine-tuning by using $W = W^{\text{res}} + AB$. This approach prioritizes training the most influential parameters, thereby accelerating
 125 convergence from the start. Inheriting LoRA’s benefits of reduced parameter count and deployment
 126 simplicity, PiSSA further leverages efficient SVD computations to expedite the training process. **This
 127 concentration of updates also motivates the output-space regularizers introduced in BA-LoRA.**
 128

129

2.2 BIAS-ALLEVIATING LOW-RANK ADAPTATION (BA-LoRA)

130 Catastrophic Inheritance refers to vulnerabilities from biases inherent in large-scale training data,
 131 particularly attribute bias and class imbalance, that degrade downstream performance, introduce
 132 unfair biases, and pose security risks. **These effects manifest during fine-tuning as three distinct
 133 subproblems: Knowledge Drift**, where the model unintentionally forgets or distorts robust pre-trained
 134 knowledge (Kirkpatrick et al., 2017); **Representation Collapse** (Bardes et al., 2021); and **Overfitting
 135 to Noise** (Chen et al., 2019). To address them, we propose BA-LoRA, a unified framework with
 136 three regularizers—consistency, diversity, and SVD—each aligned to one subproblem. Instead of
 137 constraining low-rank adapter weights, BA-LoRA regularizes the output space to directly shape
 138 functional behavior and mitigate bias, with tailored variants for NLU and NLG tasks.
 139

140

2.2.1 REGULARIZATIONS FOR NLU TASKS

141 **Consistency Regularization.** To directly combat **Knowledge Drift**, we adopt a knowledge distil-
 142 lation approach based on standard practices (Hinton et al., 2015), using the Kullback-Leibler (KL)
 143 divergence between the temperature-scaled probability distributions. Let $\mathbf{Z}_P, \mathbf{Z}_F \in \mathbb{R}^{N \times D}$ be the
 144 batch output logits from the pre-trained and fine-tuned models respectively, where N is the batch size
 145 and D is the number of classes. The loss is defined as:
 146

$$147 \quad \mathcal{L}_{\text{CR_NLU}} = T^2 \cdot \text{KL}(\text{softmax}(\mathbf{Z}_P/T) \parallel \text{softmax}(\mathbf{Z}_F/T)) \quad (4)$$

148 where T is a temperature parameter that softens the distributions. This objective encourages the
 149 fine-tuned model to mimic the nuanced decision-making process of the pre-trained model **on examples
 150 where the teacher signal is reliable**, preserving foundational knowledge. The T^2 scaling factor ensures
 151 gradient magnitudes are commensurate with standard cross-entropy loss.
 152

153 **Diversity Regularization.** To counteract **Representation Collapse**, particularly on imbalanced
 154 datasets, we promote diversity in the model’s predictions across a batch. Inspired by (Bardes et al.,
 155 2021), we regularize the batch-wise output logits to decorrelate the predictions for different classes.
 156

162 Let $\mathbf{Z}_F \in \mathbb{R}^{N \times D}$ be the logit matrix for a batch. We first center the logits and then compute the
 163 $D \times D$ covariance matrix $C(\mathbf{Z}_F)$. The regularizer penalizes the off-diagonal elements of this matrix:
 164

$$165 \quad \mathcal{L}_{\text{DR_NLU}} = \frac{1}{D} \sum_{i \neq j} [C(\mathbf{Z}_F)]_{i,j}^2 \quad (5)$$

167 where the covariance matrix is computed using its matrix form:
 168

$$169 \quad C(\mathbf{Z}_F) = \frac{1}{N-1} \mathbf{Z}_{\text{centered}}^T \mathbf{Z}_{\text{centered}}, \quad \text{where } \mathbf{Z}_{\text{centered}} = \mathbf{Z}_F - \bar{\mathbf{Z}}_F \quad (6)$$

171 Here, $\bar{\mathbf{Z}}_F$ is the matrix where each row is the mean logit vector computed over the batch. This loss
 172 **discourages excessive correlation between** the model’s predictions for any two distinct classes across
 173 the batch, thus preventing the model from collapsing towards a few dominant classes.

174 **Singular Value Decomposition Regularization.** To mitigate **Overfitting to Noise** and encourage
 175 the model to learn robust features, we introduce a regularizer that **encourages the spectral energy of**
 176 **the batch-wise output logit matrix to concentrate in its leading singular components**. Inspired by the
 177 principle that dominant singular values capture the most salient data patterns (Chen et al., 2019), this
 178 regularizer incentivizes the model to form simpler, more coherent decision boundaries for samples
 179 within a batch, rather than fitting to **high-frequency logit fluctuations that are poorly aligned with the**
 180 **task labels**. On the fine-tuned logit matrix $\mathbf{Z}_F \in \mathbb{R}^{N \times D}$, we perform SVD and maximize the ratio of
 181 spectral energy concentrated in the top- k singular values:
 182

$$183 \quad \mathcal{L}_{\text{SVDR_NLU}} = -\frac{\sum_{i=1}^k \sigma_i}{\sum_{j=1}^{\min(N,D)} \sigma_j} \quad (7)$$

184 where σ_i is the i -th largest singular value. The hyperparameter k controls the rank preference. In the
 185 NLU experiments, where the number of classes D is typically moderate, the computational cost of
 186 performing an exact SVD is minimal and poses no challenge to the training efficiency.
 187

188 **Overall Objective Function for NLU.** The overall NLU objective is formulated as follows:
 189

$$190 \quad \mathcal{L}_{\text{NLU}} = \mathcal{L}_{\text{task_NLU}} + \lambda_1 \mathcal{L}_{\text{CR_NLU}} + \lambda_2 \mathcal{L}_{\text{DR_NLU}} + \lambda_3 \mathcal{L}_{\text{SVDR_NLU}} \quad (8)$$

191 where $\mathcal{L}_{\text{task_NLU}}$ represents the standard cross-entropy loss function for the downstream task, and
 192 λ_1 , λ_2 , and λ_3 are weighting parameters to balance each regularization term’s contribution.
 193

2.2.2 REGULARIZATIONS FOR NLG TASKS

194 **Consistency Regularization.** To combat **Knowledge Drift**, we employ temperature-controlled
 195 knowledge distillation (Hinton et al., 2015), using the Kullback-Leibler Divergence (KLD) between
 196 the output distributions of the fine-tuned (student) model, \mathcal{P}_F , and the pre-trained (teacher) model,
 197 \mathcal{P}_P . A temperature parameter, T , softens these distributions, compelling the student to learn the
 198 teacher’s nuanced output, not just its top prediction, **especially on tokens where the teacher distribution**
 199 **provides a meaningful and well-calibrated soft target**. The loss is defined as:
 200

$$201 \quad \mathcal{L}_{\text{CR_NLG}} = T^2 \cdot \frac{1}{M} \sum_{i=1}^M \text{KL}(\mathcal{P}_P(y_i | \mathbf{x}; T) \| \mathcal{P}_F(y_i | \mathbf{x}; T)) \quad (9)$$

202 where for an input sequence \mathbf{x} , y_i is the target token at position i , and $\mathcal{P}(y_i | \mathbf{x}; T) = \text{softmax}(\mathbf{z}_i/T)$
 203 is the temperature-scaled conditional probability from the logit vector \mathbf{z}_i . The loss is averaged over
 204 all M valid (non-padded) tokens in the batch. The critical T^2 scaling factor maintains gradient
 205 magnitude consistency with standard distillation.
 206

207 **Diversity Regularization.** To counteract **Representation Collapse** in generation, we address a
 208 fundamental challenge: naively maximizing the entropy of the entire vocabulary distribution conflicts
 209 with the task objective of producing coherent text (Gat et al., 2020). We resolve this with a novel
 210 *focused* entropy regularizer. Inspired by Top-K sampling, our method promotes diversity exclusively
 211 within the set of most plausible candidate tokens, denoted as $\mathcal{V}_{\text{top-k}}$. For each token, we define the
 212 loss as the negative entropy computed solely within this restricted set:
 213

$$214 \quad \mathcal{L}_{\text{DR_NLG}} = -\frac{1}{M} \sum_{i=1}^M \sum_{j \in \mathcal{V}_{\text{top-k}}^{(i)}} P'_F(x_j | \mathbf{h}_i) \log P'_F(x_j | \mathbf{h}_i) \quad (10)$$

216 where $P'_F(x_j | \mathbf{h}_i)$ is the re-normalized probability from the fine-tuned model for token x_j within the
 217 set $\mathcal{V}_{\text{top-}k}^{(i)}$ for the i -th valid token, given the corresponding final hidden state \mathbf{h}_i .
 218

219 **Singular Value Decomposition Regularization.** To mitigate **Overfitting to Noise**, we regularize
 220 the structure of the batch-wise output logit matrix. Building on the principle that dominant singular
 221 values capture salient data patterns (Chen et al., 2019), we encourage a low-rank structure. For
 222 tractability with large vocabularies, we use randomized SVD (Halko et al., 2011) and normalize by
 223 the efficient Frobenius norm to avoid expensive full-spectrum computation. We thus define the loss
 224 as the negative ratio of the sum of the top- k singular values to the Frobenius norm:
 225

$$\mathcal{L}_{\text{SVDR_NLG}} = -\frac{\sum_{i=1}^k \tilde{\sigma}_i}{\|\mathbf{Z}_{\text{valid}}\|_F} \quad (11)$$

228 Here, $\tilde{\sigma}_i$ is the i -th largest approximated singular value of the valid logit matrix $\mathbf{Z}_{\text{valid}} \in \mathbb{R}^{M \times |\mathcal{V}|}$,
 229 where $|\mathcal{V}|$ is the vocabulary size, and $\|\cdot\|_F$ denotes the Frobenius norm.
 230

231 **Overall Objective Function for NLG.** Integrating these components, the final objective function
 232 for NLG tasks is a weighted sum of the task loss and our three regularization terms:
 233

$$\mathcal{L}_{\text{NLG}} = \mathcal{L}_{\text{task_NLG}} + \lambda_1 \mathcal{L}_{\text{CR_NLG}} + \lambda_2 \mathcal{L}_{\text{DR_NLG}} + \lambda_3 \mathcal{L}_{\text{SVDR_NLG}} \quad (12)$$

234 where $\mathcal{L}_{\text{task_NLG}}$ is the standard causal language modeling loss. Our experiments revealed the Mini-
 235 mal Intervention Principle: robust fine-tuning is best achieved by applying regularizers with minimal
 236 weights to gently guide the model. A detailed sensitivity analysis is provided in Appendix C.2.
 237

238 3 EXPERIMENTS

239 3.1 IMPLEMENTATION DETAILS

240 Our experimental setup is broadly aligned with recent PEFT studies (Meng et al., 2024). For NLG
 241 tasks on LLaMA-2-7B, we use the AdamW optimizer (Loshchilov & Hutter, 2017) with a learning
 242 rate of 2×10^{-5} , a cosine schedule (0.03 warmup ratio), and no weight decay. We set `lora_dropout`
 243 to 0, use BFloat16 precision, a LoRA rank (r) and alpha (α) of 128, and an effective batch size of
 244 32. The key regularization weights for our method are set to $\lambda_1 = 0.025$, $\lambda_2 = 0.005$, $\lambda_3 = 0.005$,
 245 with an SVD rank of $k = 10$. For NLU tasks on the GLUE benchmark, learning rates, batch sizes,
 246 and other core hyperparameters are task-specific to strictly align with our baseline, as detailed in
 247 the appendix. For our method in the NLU setting, we use no weight decay and set regularization
 248 hyperparameters to $\lambda_1 = 0.15$, $\lambda_2 = 0.03$, $\lambda_3 = 0.03$ with an SVD rank $k = 5$. **For each backbone,**
 249 **regularization weights are selected via coarse grid search on a held-out validation split and then kept**
 250 **fixed for that setting (see Appendices C.2 and D.1 for details).** All experiments were conducted
 251 on NVIDIA A40 GPUs and averaged over three random seeds (42, 1024, 2024). Full and detailed
 252 hyperparameter configurations for all models and tasks are available in Appendix B.
 253

254 3.2 RESULTS AND ANALYSIS

255 Table 1: Performance comparison on NLG tasks. We compare our method (BA-LoRA) against
 256 popular fine-tuning baselines, including Full Fine-tuning and various state-of-the-art parameter-
 257 efficient techniques. The best results in each column are highlighted in **bold**.
 258

Methods	GSM8K	MATH	HumanEval	MBPP	MT-Bench	Avg
Full FT	48.9 ± 0.49	7.48 ± 0.22	20.52 ± 0.29	23.64 ± 0.38	4.85 ± 0.09	21.08
LoRA	42.68 ± 0.54	5.92 ± 0.15	16.80 ± 0.38	21.51 ± 0.43	4.60 ± 0.14	18.30
AdaLoRA	41.95 ± 0.90	6.24 ± 0.38	18.10 ± 0.46	20.19 ± 0.71	4.79 ± 0.18	18.25
DoRA	41.77 ± 0.74	6.20 ± 0.48	16.86 ± 0.54	21.60 ± 0.49	4.48 ± 0.14	18.18
MiLoRA	43.09 ± 1.16	6.31 ± 0.39	17.55 ± 0.24	20.22 ± 0.37	4.50 ± 0.17	18.33
LoRA+	47.84 ± 0.39	7.21 ± 0.49	20.07 ± 0.38	23.69 ± 0.29	5.11 ± 0.06	20.78
LoRA-FA	40.25 ± 0.46	5.66 ± 0.47	15.91 ± 0.41	20.01 ± 0.32	4.67 ± 0.12	17.30
LoRA-GA	50.47 ± 0.98	7.13 ± 0.44	19.44 ± 0.45	23.05 ± 0.40	5.04 ± 0.10	21.03
PiSSA	51.48 ± 0.34	7.60 ± 0.18	19.48 ± 0.45	23.84 ± 0.46	4.92 ± 0.07	21.46
CorDA	53.90 ± 0.56	8.52 ± 0.27	21.03 ± 0.37	24.15 ± 0.44	5.15 ± 0.09	22.55
CorDA++	55.03 ± 0.52	8.95 ± 0.37	21.76 ± 0.39	24.74 ± 0.47	5.64 ± 0.12	23.22
BA-LoRA	55.86 ± 0.35	9.47 ± 0.52	23.58 ± 0.25	36.86 ± 0.31	5.11 ± 0.05	25.90

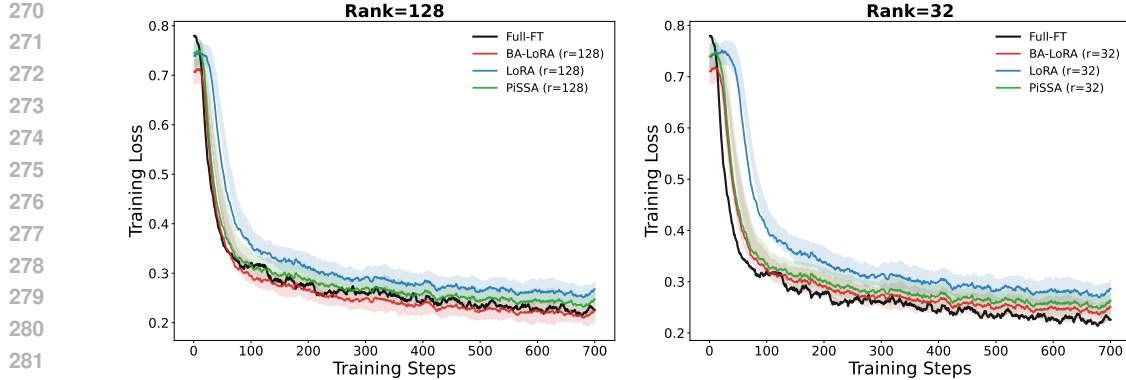


Figure 2: Training task loss of **Full Fine-Tuning (Full FT)**, LoRA, PiSSA, and BA-LoRA on MetaMath: (left) rank 128 and (right) rank 32. All curves are smoothed for visual clarity.

3.2.1 PERFORMANCE ON NLG AND NLU TASKS

To evaluate BA-LoRA on NLG tasks, we conduct a fair comparison against strong baselines (Table 1), sourcing their scores from original publications with comparable setups (see Appendix B.3). These baselines include Full Fine-tuning, LoRA (Hu et al., 2021), AdaLoRA (Zhang et al., 2023b), DoRA (Liu et al., 2024), MiLoRA (Wang et al., 2024a), LoRA+ (Hayou et al., 2024), LoRA-FA (Zhang et al., 2023a), LoRA-GA (Wang et al., 2024b), PiSSA (Meng et al., 2024), CorDA (Yang et al., 2024), and CorDA++ (Yang et al., 2025). We fine-tuned LLaMA-2-7B (Touvron et al., 2023) on MetaMathQA (Yu et al., 2023) and assessed mathematical problem-solving capabilities using the GSM8K (Cobbe et al., 2021) and MATH (Yu et al., 2023) validation sets, reporting Accuracy. Similarly, models were fine-tuned on CodeFeedback (Zheng et al., 2024) and evaluated for coding via HumanEval (Chen et al., 2021) and MBPP (Austin et al., 2021), with PASS@1 metrics reported. To assess conversational abilities, models were trained on WizardLM-Evol-Instruct (Xu et al., 2024) and evaluated on MT-Bench (Zheng et al., 2024), with response quality judged by GPT-4 and first-turn scores reported. All experiments utilized 100K data points and a single epoch for efficiency.

As shown in Table 1, BA-LoRA establishes a new state-of-the-art on LLaMA-2-7B, outperforming the strongest baselines. Specifically, compared to the highly competitive CorDA++, BA-LoRA further enhances performance on the reasoning task GSM8K by 0.83 points and the coding task HumanEval by 1.82 points. While CorDA++ maintains an edge on MT-Bench, BA-LoRA's substantial gains on other benchmarks lead to a superior average score, achieving a 2.68-point uplift over CorDA++, **with the largest margin on MBPP, a small natural language-to-code benchmark with limited test coverage and susceptibility to overfitting and spurious patterns, where BA-LoRA's output-space regularization is helpful under noisy supervision.** This performance improvement is further corroborated by the model's optimization dynamics. As illustrated in Figure 2, BA-LoRA also demonstrates superior training efficiency on the MetaMath dataset. Across both high ($r = 128$) and low ($r = 32$) ranks, our method achieves a lower final training task loss than LoRA and PiSSA, reaching levels comparable to Full FT, which we attribute to our principled regularization scheme guiding the optimization toward a more favorable solution space. **An extensive comparison across diverse model families and scales, including dense and MoE models from 7B to LLaMA-3-70B, is provided in Appendix C.3 (Figure 5).**

To assess BA-LoRA on NLU tasks, we experimented on the GLUE benchmark (Wang et al., 2018), which includes two single-sentence classification tasks (CoLA, SST), five paired-text classification tasks (MNLI, RTE, QQP, MRPC, QNLI), and one text similarity prediction task (STS-B). The evaluation metrics comprise the overall matched and mismatched accuracy for MNLI, the Matthews correlation coefficient for CoLA, the Pearson correlation coefficient for STS-B, and the accuracy for the remaining tasks. We used the DeBERTa-v3-base model (He et al., 2021) and compared BA-LoRA against eight strong baseline methods, including Full Fine-Tuning (Full FT), BitFit (Zaken et al., 2021), HAdapter (Houlsby et al., 2019), PAdapter (Pfeiffer et al., 2020), LoRA (Hu et al., 2021), DoRA (Liu et al., 2024), AdaLoRA (Zhang et al., 2023b), and PiSSA (Meng et al., 2024).

Table 2 presents the results of DeBERTa-v3-base across eight NLU tasks, demonstrating the strong overall performance of BA-LoRA. It surpasses all parameter-efficient fine-tuning (PEFT) baselines

on every task and achieves the highest average score. On average, BA-LoRA outperforms PiSSA and LoRA by 1.20 and 2.11 points, respectively. The consistent, broad-based improvements across this diverse suite of both NLG and NLU tasks provide strong evidence that our principled, three-pronged strategy not only mitigates the fundamental failure modes associated with Catastrophic Inheritance but also offers a practical route to state-of-the-art performance with parameter-efficient adaptation.

Table 2: Performance Comparison on NLU Benchmarks. We compare BA-LoRA with various PEFT baselines on the DeBERTa-v3-base model. The best result in each column is highlighted in bold.

Methods	#Params	MNLI	SST-2	MRPC	CoLA	QNLI	QQP	RTE	STS-B	Avg
Full FT	184M	90.34 \pm 0.18	96.33 \pm 0.11	89.95 \pm 1.07	71.43 \pm 0.72	94.24 \pm 0.10	92.11 \pm 0.28	83.75 \pm 1.81	91.04 \pm 0.48	88.86
BitFit	0.1M	89.54 \pm 0.29	94.68 \pm 0.11	87.95 \pm 1.33	67.31 \pm 0.49	92.45 \pm 0.17	88.72 \pm 0.45	79.12 \pm 0.39	91.63 \pm 0.37	86.43
HAdapter	1.22M	90.23 \pm 0.07	95.38 \pm 0.06	89.97 \pm 0.27	68.73 \pm 0.27	94.31 \pm 0.29	91.99 \pm 0.28	84.76 \pm 0.39	91.58 \pm 0.13	88.37
PAAdapter	1.18M	90.42 \pm 0.36	95.49 \pm 0.10	89.71 \pm 0.35	69.04 \pm 0.10	94.38 \pm 0.26	92.15 \pm 0.43	85.53 \pm 0.18	91.69 \pm 0.13	88.55
LoRA	1.33M	90.71 \pm 0.29	94.79 \pm 0.16	89.85 \pm 0.21	70.05 \pm 0.34	93.94 \pm 0.09	92.07 \pm 0.48	85.43 \pm 0.09	91.67 \pm 0.29	88.56
DoRA	1.27M	90.48 \pm 0.10	95.85 \pm 0.08	91.04 \pm 0.15	71.03 \pm 0.18	94.21 \pm 0.37	92.34 \pm 0.16	86.19 \pm 0.25	91.92 \pm 0.38	89.13
AdaLoRA	1.27M	90.87 \pm 0.08	96.18 \pm 0.43	90.81 \pm 0.40	71.64 \pm 0.12	94.68 \pm 0.46	92.37 \pm 0.35	87.78 \pm 0.36	91.97 \pm 0.43	89.53
PiSSA	1.33M	90.47 \pm 0.44	95.81 \pm 0.45	91.48 \pm 0.49	72.27 \pm 0.29	94.41 \pm 0.41	92.21 \pm 0.26	87.14 \pm 0.08	91.93 \pm 0.25	89.47
BA-LoRA	1.33M	91.26 \pm 0.49	96.25 \pm 0.09	92.11 \pm 0.55	75.46 \pm 0.62	95.35 \pm 0.14	93.63 \pm 0.52	88.58 \pm 0.73	92.71 \pm 0.38	90.67

3.2.2 MITIGATING THE EFFECTS OF NOISY PRE-TRAINING DATA

Given that large-scale pre-training corpora from web crawls are inherently noisy (Gao et al., 2020; Dodge et al., 2021), a critical challenge is ensuring that fine-tuning enhances the core signal rather than inherited noise. To investigate BA-LoRA’s ability to address this, we conduct a controlled study on models pre-trained on corpora of distinct quality. Our testbeds are RoBERTa-base (Liu et al., 2019), pre-trained on a high-quality, curated corpus, and T5-base (Raffel et al., 2020), pre-trained on the noisier, large-scale C4 web corpus.¹ While these models differ in architecture, their distinct pre-training corpora provide an ideal **but not fully controlled** testbed for evaluating robustness against inherited noise. We evaluate on a representative subset of the GLUE benchmark.

As detailed in Table 3, BA-LoRA achieves the best average performance against strong PEFT baselines. The central finding is that the advantage of BA-LoRA is significantly more pronounced on the model pre-trained on noisier data. While BA-LoRA establishes a solid 1.11-point average improvement over the strongest baseline (PiSSA) on the cleanly-trained RoBERTa-base (86.34 vs. 85.23), this performance gain nearly triples to a substantial 3.26 points on the T5-base (87.97 vs. 84.71). The pronounced disparity in improvement margin ($\Delta_{T5} = 3.26$ vs. $\Delta_{RoBERTa} = 1.11$) is **consistent with our hypothesis** that BA-LoRA is particularly beneficial for models pre-trained on noisier web corpora, **though it does not isolate architectural factors**.

3.2.3 MITIGATING REPRESENTATIONAL BIAS FROM DATA IMBALANCE

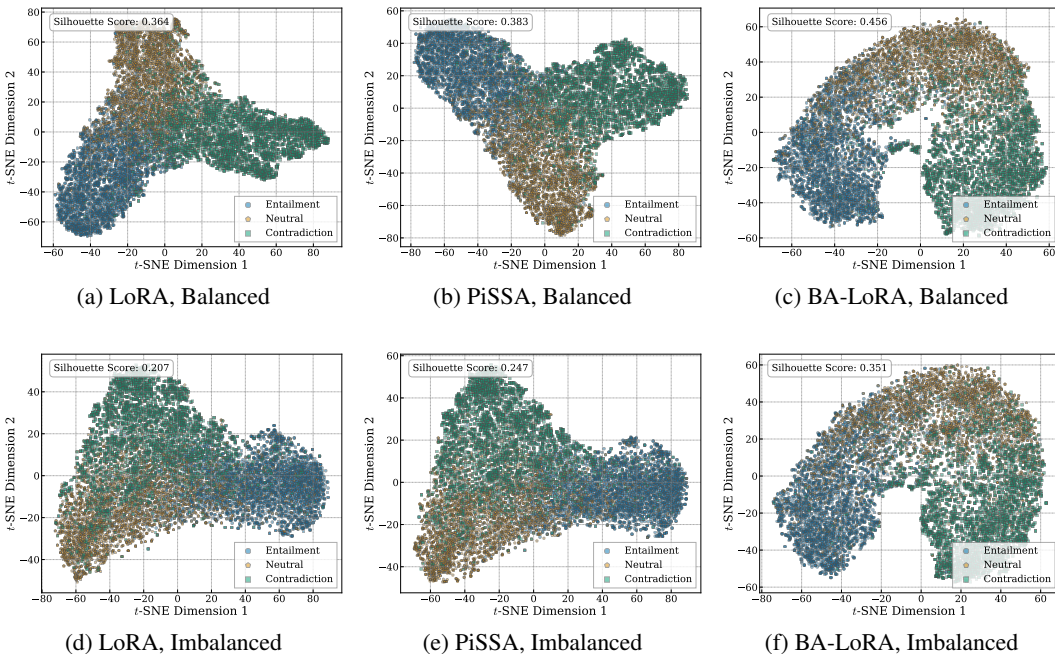
This experiment qualitatively investigates BA-LoRA’s capacity to counteract the representational degradation caused by data imbalance, which is one way Catastrophic Inheritance can manifest during downstream fine-tuning. We visualize the final hidden-layer feature representations from RoBERTa-base fine-tuned on the MNLI task using t-SNE (Van der Maaten & Hinton, 2008). As shown in Figure 3, we compare feature manifolds learned on the standard balanced dataset against those from a deliberately imbalanced version—constructed by subsampling the training data to a 100:10:1 ratio for the ‘Entailment’, ‘Neutral’, and ‘Contradiction’ classes. This controlled comparison is designed to simulate the challenge of learning from highly skewed data distributions on top of a pre-trained model, where Catastrophic Inheritance-style failures can arise.

The visualization contrasts the methods’ resilience to data imbalance. While representations from baseline LoRA and PiSSA suffer degradation and class overlap (Figure 3d,e), BA-LoRA maintains a well-separated manifold (Figure 3f; **see Table 12 in Appendix C.6 for quantitative verification**). This visualization is consistent with the effectiveness of our diversity regularizer (\mathcal{L}_{DR}) in preventing feature degradation from skewed data distributions. This effect is reinforced by the consistency (\mathcal{L}_{CR}) and SVD (\mathcal{L}_{SVDR}) regularizers, which together help the representations remain distinct and robust.

¹The C4 corpus (Colossal Clean Crawled Corpus) is derived from the broad Common Crawl web scrape via heuristic filtering. While RoBERTa’s \sim 160GB dataset also includes web text, it is a curated mixture containing high-purity sources like BooksCorpus and English Wikipedia. In contrast, C4 (\sim 750GB) is a larger, more homogeneous corpus drawn from a rawer source, making it a more representative testbed for web-scale noise.

378
 379 Table 3: Performance comparison of our method (BA-LoRA) against PEFT baselines (LoRA, PiSSA)
 380 on RoBERTa-base and T5-base. Models are evaluated on a subset of the GLUE benchmark. The best
 381 result for each model is in bold.
 382

Model	Methods	MNLI	SST-2	CoLA	QNLI	MRPC	Avg
RoBERTa-base	LoRA	85.63 ± 0.01	94.03 ± 0.02	62.40 ± 0.71	91.37 ± 0.97	87.98 ± 0.23	84.28
	PiSSA	85.72 ± 0.40	93.64 ± 0.13	67.28 ± 0.59	91.40 ± 0.54	88.11 ± 0.24	85.23
	BA-LoRA	86.59 ± 0.58	94.83 ± 0.45	67.91 ± 0.21	92.28 ± 0.37	90.07 ± 0.32	86.34
T5-base	LoRA	85.30 ± 0.04	94.04 ± 0.11	69.35 ± 0.05	92.96 ± 0.09	68.38 ± 0.01	82.08
	PiSSA	85.75 ± 0.07	94.07 ± 0.06	74.27 ± 0.39	93.15 ± 0.14	76.31 ± 0.51	84.71
	BA-LoRA	86.91 ± 0.48	95.20 ± 0.29	80.19 ± 1.03	94.12 ± 0.32	83.43 ± 0.71	87.97



410 Figure 3: t-SNE visualizations of features from RoBERTa-base fine-tuned with LoRA, PiSSA, and
 411 BA-LoRA on the MNLI task under balanced (top) and imbalanced (bottom) settings.
 412

413 3.2.4 ABLATION STUDY

414 Our ablation study (Table 4) empirically supports our principled deconstruction of Catastrophic
 415 Inheritance. On NLG tasks with the LLaMA-2-7B model, we observe a consistent pattern: each
 416 regularizer yields a positive contribution over the baseline ('w/o Reg'). Specifically, gains from
 417 the consistency regularizer (\mathcal{L}_{CR}) support its role in combating Knowledge Drift by preserving
 418 foundational knowledge. Similarly, improvements from the diversity regularizer (\mathcal{L}_{DR}) highlight the
 419 importance of preventing Representation Collapse, and the significant contribution from the SVD
 420 regularizer (\mathcal{L}_{SVDR}) confirms the benefit of mitigating Overfitting to Noise.
 421

422 This trend is mirrored in NLU tasks, where the DeBERTa-v3-base model also shows a clear uplift
 423 with each regularizer over the baseline. The full BA-LoRA model, which synergistically combines
 424 all three components, consistently achieves the highest performance across all evaluated settings. In
 425 summary, these results provide strong evidence that Knowledge Drift, Representation Collapse, and
 426 Overfitting to Noise are important and complementary failure modes in fine-tuning. Consequently,
 427 our integrated, multi-pronged solution yields strong generalization and robustness across both NLU
 428 and NLG domains. The selection of our regularization coefficients ($\lambda_1, \lambda_2, \lambda_3$) is validated by a
 429 detailed sensitivity analysis in Figure 4, and Table 10 further shows that the same regularization
 430 framework consistently improves multiple LoRA-style methods (LoRA, DoRA, PiSSA).
 431

3.2.5 COMPUTATIONAL COST ANALYSIS

432 Table 4: Ablation study of BA-LoRA regularizations on GSM8K, MATH, and NLU tasks. Results
 433 on GSM8K and MATH are from LLaMA-2-7B, while the NLU task refers to the average GLUE
 434 score from DeBERTa-v3-base. "Baseline" (PiSSA) is fine-tuned without our proposed regularizations.
 435 \mathcal{L}_{CR} , \mathcal{L}_{DR} , and $\mathcal{L}_{\text{SVDR}}$ denote adding only a single corresponding regularization to the baseline.
 436 "BA-LoRA (Full)" is the full model using all regularizations.

Configuration	GSM8K	MATH	Average of GLUE
Baseline (PiSSA)	51.48 ± 0.34	7.60 ± 0.18	89.47
\mathcal{L}_{CR}	54.25 ± 0.59	9.15 ± 0.25	90.18
\mathcal{L}_{DR}	53.60 ± 0.46	8.95 ± 0.18	89.85
$\mathcal{L}_{\text{SVDR}}$	52.95 ± 0.55	8.70 ± 0.22	89.71
BA-LoRA (Full)	55.86 ± 0.35	9.47 ± 0.52	90.67

444 To quantitatively evaluate the computational efficiency and performance of our method, we conducted a comparative experiment on two A40
 445 (48GB) GPUs using DeepSpeed (Rasley et al.,
 446 2020) ZeRO-2 optimization. We fine-tuned the
 447 LLaMA-2-7B model on the first 100,000 entries
 448 of the MetaMathQA dataset. This experiment
 449 benchmarked four methods: full fine-tuning
 450 (Full FT), LoRA, PiSSA, and our proposed BA-
 451 LoRA. For each method, we measured the peak
 452 GPU memory consumption and the total training time to assess computational cost. Model perfor-
 453 mance was subsequently evaluated on the GSM8K benchmark.

454 The results in Table 5 quantify the performance-cost trade-offs of various methods. BA-LoRA sets a
 455 new state-of-the-art with a GSM8K score of 55.86, significantly outperforming all baselines. This
 456 substantial performance gain is achieved with a modest overhead compared to PiSSA (+10.75 GB
 457 memory, +31 min training), highlighting a compelling performance-cost balance.

4 RELATED WORK

463 Our work bridges two critical research areas. **In Parameter-Efficient Fine-Tuning (PEFT)**, our
 464 method builds upon Low-Rank Adaptation (LoRA) (Hu et al., 2021). Numerous LoRA variants
 465 have focused on enhancing performance and efficiency, such as QLoRA (Dettmers et al., 2024) and
 466 PiSSA (Meng et al., 2024). Crucially, while recent work has identified LoRA’s low-rank update
 467 as a potential bottleneck that can interfere with pre-trained knowledge (Zhang et al., 2023a), the
 468 systematic mitigation of inherited biases remains a significant gap (see Appendix A.4). **In Bias**
 469 **Mitigation**, addressing biases from web-scale corpora is a foundational concern (Bender et al., 2021).
 470 While a rich literature exists on data filtering (Dodge et al., 2021) and algorithmic adjustments for full
 471 fine-tuning—such as representation debiasing (Ravfogel et al., 2020) and decoding strategies (Sheng
 472 et al., 2019) (see (Gallegos et al., 2024) for a survey)—these are not directly applicable to PEFT.
 473 Although recent analyses have begun to probe fairness issues within PEFT (Ding et al., 2024),
 474 BA-LoRA is, to our knowledge, the first to propose a concrete, multi-faceted algorithmic framework.
 475 It moves beyond analysis to systematically mitigate the broader problem of Catastrophic Inheritance
 476 by integrating a principled regularization scheme directly into the LoRA-based process.

5 CONCLUSION

477 This paper introduces BA-LoRA, a novel parameter-efficient fine-tuning framework aimed at mitigat-
 478 ing Catastrophic Inheritance. Our core contribution is a principled approach that decomposes this
 479 challenge into three sub-problems—Knowledge Drift, Representation Collapse, and Overfitting to
 480 Noise—and addresses them with three targeted regularizers. Extensive experiments across NLG and
 481 NLU benchmarks support our integrated strategy, which achieves strong performance and improves
 482 robustness to inherited data biases relative to standard LoRA variants. By addressing Catastrophic
 483 Inheritance explicitly within the LoRA framework, BA-LoRA offers a more reliable pathway to adapt
 484 pre-trained models to downstream tasks where robustness and fairness are important.

486 REFERENCES
487

488 AI@Meta. Llama 3 model card. 2024. URL https://github.com/meta-llama/llama3/blob/main/MODEL_CARD.md.

489

490 Jacob Austin, Augustus Odena, Maxwell Nye, Maarten Bosma, Henryk Michalewski, David Dohan,
491 Ellen Jiang, Carrie Cai, Michael Terry, Quoc Le, et al. Program synthesis with large language
492 models. *arXiv preprint arXiv:2108.07732*, 2021.

493

494 Jinze Bai, Shuai Bai, Yunfei Chu, Zeyu Cui, Kai Dang, Xiaodong Deng, Yang Fan, Wenbin Ge,
495 Yu Han, Fei Huang, Binyuan Hui, Luo Ji, Mei Li, Junyang Lin, Runji Lin, Dayiheng Liu, Gao Liu,
496 Chengqiang Lu, Keming Lu, Jianxin Ma, Rui Men, Xingzhang Ren, Xuancheng Ren, Chuanchi Tan,
497 Sinan Tan, Jianhong Tu, Peng Wang, Shijie Wang, Wei Wang, Shengguang Wu, Benfeng Xu, Jin
498 Xu, An Yang, Hao Yang, Jian Yang, Shusheng Yang, Yang Yao, Bowen Yu, Hongyi Yuan, Zheng
499 Yuan, Jianwei Zhang, Xingxuan Zhang, Yichang Zhang, Zhenru Zhang, Chang Zhou, Jingren Zhou,
500 Xiaohuan Zhou, and Tianhang Zhu. Qwen technical report. *arXiv preprint arXiv:2309.16609*,
501 2023.

502

503 Adrien Bardes, Jean Ponce, and Yann LeCun. Vicreg: Variance-invariance-covariance regularization
504 for self-supervised learning. *arXiv preprint arXiv:2105.04906*, 2021.

505

506 Solon Barocas and Andrew D Selbst. Big data's disparate impact. *Calif. L. Rev.*, 104:671, 2016.

507

508 Emily M Bender, Timnit Gebru, Angelina McMillan-Major, and Shmargaret Shmitchell. On the
509 dangers of stochastic parrots: Can language models be too big? In *Proceedings of the 2021 ACM
510 conference on fairness, accountability, and transparency*, pp. 610–623, 2021.

511

512 Abeba Birhane and Vinay Uday Prabhu. Large image datasets: A pyrrhic win for computer vision?
513 In *2021 IEEE Winter Conference on Applications of Computer Vision (WACV)*, pp. 1536–1546.
514 IEEE, 2021.

515

516 Rishi Bommasani, Drew A Hudson, Ehsan Adeli, Russ Altman, Simran Arora, Sydney von Arx,
517 Michael S Bernstein, Jeannette Bohg, Antoine Bosselut, Emma Brunskill, et al. On the opportuni-
518 ties and risks of foundation models. *arXiv preprint arXiv:2108.07258*, 2021.

519

520 Nicholas Carlini, Daphne Ippolito, Matthew Jagielski, Katherine Lee, Florian Tramer, and
521 Chiyuan Zhang. Quantifying memorization across neural language models. *arXiv preprint
522 arXiv:2202.07646*, 2022.

523

524 Nicholas Carlini, Matthew Jagielski, Christopher A Choquette-Choo, Daniel Paleka, Will Pearce,
525 Hyrum Anderson, Andreas Terzis, Kurt Thomas, and Florian Tramèr. Poisoning web-scale training
526 datasets is practical. *arXiv preprint arXiv:2302.10149*, 2023.

527

528 Isaac Caswell, Julia Kreutzer, Lisa Wang, Ahsan Wahab, Daan van Esch, Nasanbayar Ulzii-Orshikh,
529 Allahsera Tapo, Nishant Subramani, Artem Sokolov, Claytone Sikasote, et al. Quality at a glance:
530 An audit of web-crawled multilingual datasets. *arXiv e-prints*, pp. arXiv–2103, 2021.

531

532 Yupeng Chang, Xu Wang, Jindong Wang, Yuan Wu, Linyi Yang, Kaijie Zhu, Hao Chen, Xiaoyuan
533 Yi, Cunxiang Wang, Yidong Wang, et al. A survey on evaluation of large language models. *ACM
534 Transactions on Intelligent Systems and Technology*, 15(3):1–45, 2024.

535

536 Hao Chen, Jindong Wang, Ankit Shah, Ran Tao, Hongxin Wei, Xing Xie, Masashi Sugiyama, and
537 Bhiksha Raj. Understanding and mitigating the label noise in pre-training on downstream tasks.
538 *arXiv preprint arXiv:2309.17002*, 2023.

539

540 Hao Chen, Bhiksha Raj, Xing Xie, and Jindong Wang. On catastrophic inheritance of large foundation
541 models. *arXiv preprint arXiv:2402.01909*, 2024a.

542

543 Hao Chen, Jindong Wang, Ankit Shah, Ran Tao, Hongxin Wei, Xing Xie, Masashi Sugiyama, and
544 Bhiksha Raj. Understanding and mitigating the label noise in pre-training on downstream tasks,
545 2024b.

546

547 Hao Chen, Zihan Wang, Ran Tao, Hongxin Wei, Xing Xie, Masashi Sugiyama, Bhiksha Raj, and
548 Jindong Wang. Impact of noisy supervision in foundation model learning. *IEEE Transactions on
549 Pattern Analysis and Machine Intelligence*, 2025.

540 Haolin Chen and Philip N Garner. Bayesian parameter-efficient fine-tuning for overcoming catastrophic forgetting. *IEEE/ACM Transactions on Audio, Speech, and Language Processing*, 2024.

541

542

543 Mark Chen, Jerry Tworek, Heewoo Jun, Qiming Yuan, Henrique Ponde de Oliveira Pinto, Jared Kaplan, Harri Edwards, Yuri Burda, Nicholas Joseph, Greg Brockman, Alex Ray, Raul Puri, Gretchen Krueger, Michael Petrov, Heidy Khlaaf, Girish Sastry, Pamela Mishkin, Brooke Chan, Scott Gray, Nick Ryder, Mikhail Pavlov, Alethea Power, Lukasz Kaiser, Mohammad Bavarian, Clemens Winter, Philippe Tillet, Felipe Petroski Such, Dave Cummings, Matthias Plappert, Fotios Chantzis, Elizabeth Barnes, Ariel Herbert-Voss, William Hebbgen Guss, Alex Nichol, Alex Paino, Nikolas Tezak, Jie Tang, Igor Babuschkin, Suchir Balaji, Shantanu Jain, William Saunders, Christopher Hesse, Andrew N. Carr, Jan Leike, Josh Achiam, Vedant Misra, Evan Morikawa, Alec Radford, Matthew Knight, Miles Brundage, Mira Murati, Katie Mayer, Peter Welinder, Bob McGrew, Dario Amodei, Sam McCandlish, Ilya Sutskever, and Wojciech Zaremba. Evaluating large language models trained on code, 2021.

544

545

546

547

548

549

550

551

552

553

554 Xinyang Chen, Sinan Wang, Mingsheng Long, and Jianmin Wang. Transferability vs. discriminability: Batch spectral penalization for adversarial domain adaptation. In *International conference on machine learning*, pp. 1081–1090. PMLR, 2019.

555

556

557 Karl Cobbe, Vineet Kosaraju, Mohammad Bavarian, Mark Chen, Heewoo Jun, Lukasz Kaiser, Matthias Plappert, Jerry Tworek, Jacob Hilton, Reiichiro Nakano, Christopher Hesse, and John Schulman. Training verifiers to solve math word problems. *arXiv preprint arXiv:2110.14168*, 2021.

558

559

560

561

562 Thomas M Cover. *Elements of information theory*. John Wiley & Sons, 1999.

563

564

565

566

567

568

569

570

571

572

573

574

575

576

577

578

579

580

581

582

583

584

585

586

587

588

589

590

591

592

593

Damai Dai, Chengqi Deng, Chenggang Zhao, RX Xu, Huazuo Gao, Deli Chen, Jiashi Li, Wangding Zeng, Xingkai Yu, Y Wu, et al. Deepseekmoe: Towards ultimate expert specialization in mixture-of-experts language models. *arXiv preprint arXiv:2401.06066*, 2024.

Tim Dettmers, Artidoro Pagnoni, Ari Holtzman, and Luke Zettlemoyer. Qlora: Efficient finetuning of quantized llms. *Advances in Neural Information Processing Systems*, 36, 2024.

Zhoujie Ding, Ken Ziyu Liu, Pura Peetathawatchai, Berivan Isik, and Sanmi Koyejo. On fairness of low-rank adaptation of large models, 2024. URL <https://arxiv.org/abs/2405.17512>.

Jesse Dodge, Maarten Sap, Ana Marasović, William Agnew, Gabriel Ilharco, Dirk Groeneveld, Margaret Mitchell, and Matt Gardner. Documenting large webtext corpora: A case study on the colossal clean crawled corpus. *arXiv preprint arXiv:2104.08758*, 2021.

Guanting Dong, Hongyi Yuan, Keming Lu, Chengpeng Li, Mingfeng Xue, Dayiheng Liu, Wei Wang, Zheng Yuan, Chang Zhou, and Jingren Zhou. How abilities in large language models are affected by supervised fine-tuning data composition. *arXiv preprint arXiv:2310.05492*, 2023.

Yanai Elazar, Akshita Bhagia, Ian Magnusson, Abhilasha Ravichander, Dustin Schwenk, Alane Suhr, Pete Walsh, Dirk Groeneveld, Luca Soldaini, Sameer Singh, et al. What’s in my big data? *arXiv preprint arXiv:2310.20707*, 2023.

Lijie Fan, Kaifeng Chen, Dilip Krishnan, Dina Katahi, Phillip Isola, and Yonglong Tian. Scaling laws of synthetic images for model training... for now. In *Proceedings of the IEEE/CVF Conference on Computer Vision and Pattern Recognition*, pp. 7382–7392, 2024.

Benoît Frénay and Michel Verleysen. Classification in the presence of label noise: a survey. *IEEE transactions on neural networks and learning systems*, 25(5):845–869, 2013.

Isabel O Gallegos, Ryan A Rossi, Joe Barrow, Md Mehrab Tanjim, Sungchul Kim, Franck Dernoncourt, Tong Yu, Ruiyi Zhang, and Nesreen K Ahmed. Bias and fairness in large language models: A survey. *Computational Linguistics*, 50(3):1097–1179, 2024.

Leo Gao, Stella Biderman, Sid Black, Laurence Golding, Travis Hoppe, Charles Foster, Jason Phang, Horace He, Anish Thite, Noa Nabeshima, et al. The pile: An 800gb dataset of diverse text for language modeling. *arXiv preprint arXiv:2101.00027*, 2020.

594 Itai Gat, Idan Schwartz, Alexander Schwing, and Tamir Hazan. Removing bias in multi-modal
 595 classifiers: Regularization by maximizing functional entropies. *Advances in Neural Information
 596 Processing Systems*, 33:3197–3208, 2020.

597

598 Nathan Halko, Per-Gunnar Martinsson, and Joel A Tropp. Finding structure with randomness:
 599 Probabilistic algorithms for constructing approximate matrix decompositions. *SIAM review*, 53(2):
 600 217–288, 2011.

601 Zeyu Han, Chao Gao, Jinyang Liu, Sai Qian Zhang, et al. Parameter-efficient fine-tuning for large
 602 models: A comprehensive survey. *arXiv preprint arXiv:2403.14608*, 2024.

603

604 Soufiane Hayou, Nikhil Ghosh, and Bin Yu. Lora+: Efficient low rank adaptation of large models.
 605 *arXiv preprint arXiv:2402.12354*, 2024.

606

607 Pengcheng He, Jianfeng Gao, and Weizhu Chen. Debertav3: Improving deberta using electra-style
 608 pre-training with gradient-disentangled embedding sharing, 2021.

609

610 Danny Hernandez, Tom Brown, Tom Conerly, Nova DasSarma, Dawn Drain, Sheer El-Showk, Nelson
 611 Elhage, Zac Hatfield-Dodds, Tom Henighan, Tristan Hume, et al. Scaling laws and interpretability
 612 of learning from repeated data. *arXiv preprint arXiv:2205.10487*, 2022.

613

614 Geoffrey Hinton, Oriol Vinyals, and Jeff Dean. Distilling the knowledge in a neural network. *arXiv
 preprint arXiv:1503.02531*, 2015.

615

616 Neil Houlsby, Andrei Giurgiu, Stanislaw Jastrzebski, Bruna Morrone, Quentin De Laroussilhe,
 617 Andrea Gesmundo, Mona Attariyan, and Sylvain Gelly. Parameter-efficient transfer learning for
 618 nlp. In *International conference on machine learning*, pp. 2790–2799. PMLR, 2019.

619

620 Edward J. Hu, Yelong Shen, Phillip Wallis, Zeyuan Allen-Zhu, Yuanzhi Li, Shean Wang, Lu Wang,
 621 and Weizhu Chen. Lora: Low-rank adaptation of large language models, 2021.

622

623 Albert Q Jiang, Alexandre Sablayrolles, Arthur Mensch, Chris Bamford, Devendra Singh Chaplot,
 624 Diego de las Casas, Florian Bressand, Gianna Lengyel, Guillaume Lample, Lucile Saulnier, et al.
 625 Mistral 7b. *arXiv preprint arXiv:2310.06825*, 2023.

626

627 Albert Q Jiang, Alexandre Sablayrolles, Antoine Roux, Arthur Mensch, Blanche Savary, Chris
 628 Bamford, Devendra Singh Chaplot, Diego de las Casas, Emma Bou Hanna, Florian Bressand, et al.
 629 Mixtral of experts. *arXiv preprint arXiv:2401.04088*, 2024.

630

631 Jiale Kang and Qingyu Yin. Balancing lora performance and efficiency with simple shard sharing,
 632 2025. URL <https://arxiv.org/abs/2409.15371>.

633

634 James Kirkpatrick, Razvan Pascanu, Neil Rabinowitz, Joel Veness, Guillaume Desjardins, Andrei A
 635 Rusu, Kieran Milan, John Quan, Tiago Ramalho, Agnieszka Grabska-Barwinska, et al. Overcoming
 636 catastrophic forgetting in neural networks. *Proceedings of the national academy of sciences*, 114
 637 (13):3521–3526, 2017.

638

639 Brian Lester, Rami Al-Rfou, and Noah Constant. The power of scale for parameter-efficient prompt
 640 tuning, 2021.

641

642 Shih-Yang Liu, Chien-Yi Wang, Hongxu Yin, Pavlo Molchanov, Yu-Chiang Frank Wang, Kwang-
 643 Ting Cheng, and Min-Hung Chen. Dora: Weight-decomposed low-rank adaptation. *arXiv preprint
 644 arXiv:2402.09353*, 2024.

645

646 Yinhan Liu, Myle Ott, Naman Goyal, Jingfei Du, Mandar Joshi, Danqi Chen, Omer Levy, Mike
 647 Lewis, Luke Zettlemoyer, and Veselin Stoyanov. Roberta: A robustly optimized bert pretraining
 648 approach. *arXiv preprint arXiv:1907.11692*, 2019.

649

650 Zhuang Liu and Kaiming He. A decade’s battle on dataset bias: Are we there yet? *arXiv preprint
 651 arXiv:2403.08632*, 2024.

652

653 Ilya Loshchilov and Frank Hutter. Decoupled weight decay regularization. *arXiv preprint
 654 arXiv:1711.05101*, 2017.

648 Ilya Loshchilov and Frank Hutter. Decoupled weight decay regularization, 2019.
 649

650 Alex Mallen, Akari Asai, Victor Zhong, Rajarshi Das, Daniel Khashabi, and Hannaneh Hajishirzi.
 651 When not to trust language models: Investigating effectiveness of parametric and non-parametric
 652 memories. *arXiv preprint arXiv:2212.10511*, 2022.

653 Fanxu Meng, Zhaoxi Wang, and Muhan Zhang. Pissa: Principal singular values and singular vectors
 654 adaptation of large language models, 2024.

655

656 Curtis G. Northcutt, Lu Jiang, and Isaac L. Chuang. Confident learning: Estimating uncertainty in
 657 dataset labels. *Journal of Artificial Intelligence Research (JAIR)*, 70:1373–1411, 2021.

658 OpenAI. Gpt-4 technical report, 2023.

659

660 Long Ouyang, Jeffrey Wu, Xu Jiang, Diogo Almeida, Carroll Wainwright, Pamela Mishkin, Chong
 661 Zhang, Sandhini Agarwal, Katarina Slama, Alex Ray, et al. Training language models to follow
 662 instructions with human feedback. *Advances in neural information processing systems*, 35:27730–
 663 27744, 2022.

664

665 Shubham Parashar, Zhiqiu Lin, Tian Liu, Xiangjue Dong, Yanan Li, Deva Ramanan, James Caverlee,
 666 and Shu Kong. The neglected tails in vision-language models. In *Proceedings of the IEEE/CVF
 667 Conference on Computer Vision and Pattern Recognition*, pp. 12988–12997, 2024.

668

669 Guilherme Penedo, Quentin Malartic, Daniel Hesslow, Ruxandra Cojocaru, Alessandro Cappelli,
 670 Hamza Alobeidli, Baptiste Pannier, Ebtesam Almazrouei, and Julien Launay. The refinedweb
 671 dataset for falcon llm: outperforming curated corpora with web data, and web data only. *arXiv
 preprint arXiv:2306.01116*, 2023.

672

673 Jonas Pfeiffer, Aishwarya Kamath, Andreas Rücklé, Kyunghyun Cho, and Iryna Gurevych. Adapter-
 674 fusion: Non-destructive task composition for transfer learning. *arXiv preprint arXiv:2005.00247*,
 675 2020.

676

677 Xiangyu Qi, Yi Zeng, Tinghao Xie, Pin-Yu Chen, Ruoxi Jia, Prateek Mittal, and Peter Henderson.
 678 Fine-tuning aligned language models compromises safety, even when users do not intend to! *arXiv
 preprint arXiv:2310.03693*, 2023.

679

680 Colin Raffel, Noam Shazeer, Adam Roberts, Katherine Lee, Sharan Narang, Michael Matena, Yanqi
 681 Zhou, Wei Li, and Peter J Liu. Exploring the limits of transfer learning with a unified text-to-text
 682 transformer. *Journal of machine learning research*, 21(140):1–67, 2020.

683

684 Jeff Rasley, Samyam Rajbhandari, Olatunji Ruwase, and Yuxiong He. Deepspeed: System opti-
 685 mizations enable training deep learning models with over 100 billion parameters. In *SIGKDD*, pp.
 3505–3506, 2020.

686

687 Shauli Ravfogel, Yanai Elazar, Hila Gonen, Michael Twiton, and Yoav Goldberg. Null it out:
 688 Guarding protected attributes by iterative nullspace projection. *arXiv preprint arXiv:2004.07667*,
 689 2020.

690

691 Manley Roberts, Himanshu Thakur, Christine Herlihy, Colin White, and Samuel Dooley. Data
 692 contamination through the lens of time. *arXiv preprint arXiv:2310.10628*, 2023.

693

694 Rylan Schaeffer. Pretraining on the test set is all you need. *arXiv preprint arXiv:2309.08632*, 2023.

695

696 Emily Sheng, Kai-Wei Chang, Premkumar Natarajan, and Nanyun Peng. The woman worked as a
 697 babysitter: On biases in language generation. *arXiv preprint arXiv:1909.01326*, 2019.

698

699 James Seale Smith, Yen-Chang Hsu, Lingyu Zhang, Ting Hua, Zsolt Kira, Yilin Shen, and Hongxia
 700 Jin. Continual diffusion: Continual customization of text-to-image diffusion with c-lora. *arXiv
 preprint arXiv:2304.06027*, 2023.

701

702 Hwanjun Song, Minseok Kim, Dongmin Park, Yooju Shin, and Jae-Gil Lee. Learning from noisy
 703 labels with deep neural networks: A survey. *IEEE transactions on neural networks and learning
 704 systems*, 34(11):8135–8153, 2022.

702 Lichao Sun, Yue Huang, Haoran Wang, Siyuan Wu, Qihui Zhang, Chujie Gao, Yixin Huang, Wenhan
 703 Lyu, Yixuan Zhang, Xiner Li, et al. Trustllm: Trustworthiness in large language models. *arXiv*
 704 *preprint arXiv:2401.05561*, 2024.

705

706 Gemma Team, Thomas Mesnard, Cassidy Hardin, Robert Dadashi, Surya Bhupatiraju, Shreya Pathak,
 707 Laurent Sifre, Morgane Rivière, Mihir Sanjay Kale, Juliette Love, et al. Gemma: Open models
 708 based on gemini research and technology. *arXiv preprint arXiv:2403.08295*, 2024.

709

710 Hugo Touvron, Louis Martin, Kevin Stone, Peter Albert, Amjad Almahairi, Yasmine Babaei, Nikolay
 711 Bashlykov, Soumya Batra, Prajjwal Bhargava, Shruti Bhosale, et al. Llama 2: Open foundation
 712 and fine-tuned chat models. *arXiv preprint arXiv:2307.09288*, 2023.

713

714 Laurens Van der Maaten and Geoffrey Hinton. Visualizing data using t-sne. *Journal of machine
 learning research*, 9(11), 2008.

715

716 Alex Wang, Amanpreet Singh, Julian Michael, Felix Hill, Omer Levy, and Samuel R Bowman. Glue:
 717 A multi-task benchmark and analysis platform for natural language understanding. In *International
 718 Conference on Learning Representations*, 2018.

719

720 Hanqing Wang, Yixia Li, Shuo Wang, Guanhua Chen, and Yun Chen. Milora: Harnessing minor
 721 singular components for parameter-efficient llm finetuning. *arXiv preprint arXiv:2406.09044*,
 722 2024a.

723

724 Shaowen Wang, Linxi Yu, and Jian Li. Lora-ga: Low-rank adaptation with gradient approximation.
 725 *Advances in Neural Information Processing Systems*, 37:54905–54931, 2024b.

726

727 Can Xu, Qingfeng Sun, Kai Zheng, Xiubo Geng, Pu Zhao, Jiazhan Feng, Chongyang Tao, Qingwei
 728 Lin, and Daxin Jiang. Wizardlm: Empowering large pre-trained language models to follow complex
 729 instructions. In *The Twelfth International Conference on Learning Representations*, 2024.

730

731 Hu Xu, Saining Xie, Xiaoqing Ellen Tan, Po-Yao Huang, Russell Howes, Vasu Sharma, Shang-Wen
 732 Li, Gargi Ghosh, Luke Zettlemoyer, and Christoph Feichtenhofer. Demystifying clip data. *arXiv
 733 preprint arXiv:2309.16671*, 2023.

734

735 Yibo Yang, Xiaojie Li, Zhongzhu Zhou, Shuaiwen Song, Jianlong Wu, Liqiang Nie, and Bernard
 736 Ghanem. Corda: Context-oriented decomposition adaptation of large language models for task-
 737 aware parameter-efficient fine-tuning. *Advances in Neural Information Processing Systems*, 37:
 738 71768–71791, 2024.

739

740 Yibo Yang, Sihao Liu, Chuan Rao, Bang An, Tiancheng Shen, Philip HS Torr, Ming-Hsuan Yang, and
 741 Bernard Ghanem. Dynamic context-oriented decomposition for task-aware low-rank adaptation
 742 with less forgetting and faster convergence. *arXiv preprint arXiv:2506.13187*, 2025.

743

744 Alex Young, Bei Chen, Chao Li, Chengen Huang, Ge Zhang, Guanwei Zhang, Heng Li, Jiangcheng
 745 Zhu, Jianqun Chen, Jing Chang, et al. Yi: Open foundation models by 01. ai. *arXiv preprint
 746 arXiv:2403.04652*, 2024.

747

748 Longhui Yu, Weisen Jiang, Han Shi, Jincheng Yu, Zhengying Liu, Yu Zhang, James T Kwok, Zhenguo
 749 Li, Adrian Weller, and Weiyang Liu. Metamath: Bootstrap your own mathematical questions for
 750 large language models. *arXiv preprint arXiv:2309.12284*, 2023.

751

752 Elad Ben Zaken, Shauli Ravfogel, and Yoav Goldberg. Bitfit: Simple parameter-efficient fine-tuning
 753 for transformer-based masked language-models. *arXiv preprint arXiv:2106.10199*, 2021.

754

755 Jure Zbontar, Li Jing, Ishan Misra, Yann LeCun, and Stéphane Deny. Barlow twins: Self-supervised
 756 learning via redundancy reduction. In *International conference on machine learning*, pp. 12310–
 757 12320. PMLR, 2021.

758

759 Longteng Zhang, Lin Zhang, Shaohuai Shi, Xiaowen Chu, and Bo Li. Lora-fa: Memory-efficient
 760 low-rank adaptation for large language models fine-tuning. *arXiv preprint arXiv:2308.03303*,
 761 2023a.

756 Qingru Zhang, Minshuo Chen, Alexander Bukharin, Nikos Karampatziakis, Pengcheng He, Yu Cheng,
757 Weizhu Chen, and Tuo Zhao. Adalora: Adaptive budget allocation for parameter-efficient fine-
758 tuning. *arXiv preprint arXiv:2303.10512*, 2023b.

759 Wayne Xin Zhao, Kun Zhou, Junyi Li, Tianyi Tang, Xiaolei Wang, Yupeng Hou, Yingqian Min,
760 Beichen Zhang, Junjie Zhang, Zican Dong, et al. A survey of large language models. *arXiv
761 preprint arXiv:2303.18223*, 2023.

762 Lianmin Zheng, Wei-Lin Chiang, Ying Sheng, Siyuan Zhuang, Zhanghao Wu, Yonghao Zhuang,
763 Zi Lin, Zhuohan Li, Dacheng Li, Eric Xing, et al. Judging llm-as-a-judge with mt-bench and
764 chatbot arena. *Advances in Neural Information Processing Systems*, 36, 2024.

765 Beier Zhu, Kaihua Tang, Qianru Sun, and Hanwang Zhang. Generalized logit adjustment: Calibrating
766 fine-tuned models by removing label bias in foundation models. *Advances in Neural Information
767 Processing Systems*, 36, 2024.

768 Andy Zou, Zifan Wang, J Zico Kolter, and Matt Fredrikson. Universal and transferable adversarial
769 attacks on aligned language models. *arXiv preprint arXiv:2307.15043*, 2023.

770

771

772

773

774

775

776

777

778

779

780

781

782

783

784

785

786

787

788

789

790

791

792

793

794

795

796

797

798

799

800

801

802

803

804

805

806

807

808

809

810 811 812 813 814 815 816 817 818 819 820 821 822 823 824 825 826 827 828 829 830 831 832 833 834 835 836 837 838 839 840 841 842 843 844 845 846 847 848 849 850 851 852 853 854 855 856 857 858 859 860 861 862 863 Appendix

CONTENTS

A Background	16
A.1 Challenges of Bias and Noise in Pre-training Data	16
A.2 Mitigating Bias through Parameter-Efficient Fine-Tuning	17
A.3 Typologies of Noise in Pre-training Data	17
A.4 Extended Related Work	17
B Experimental Setup	18
B.1 Models	18
B.2 Tasks, Datasets, and Metrics	18
B.3 Implementation and Training Details	19
B.4 Hyperparameter Settings	20
C More Experiments	21
C.1 Generality of the Regularization Framework	21
C.2 Hyperparameter Sensitivity Analysis	21
C.3 Analysis Across Diverse Model Architectures and Scales	22
C.4 Performance Analysis Across Different Ranks	22
C.5 Comparison of Regularization Objectives for NLU	23
C.6 Quantitative Analysis of Cluster Quality and Minority Representation	23
D More Discussions	24
D.1 Practical Hyperparameter Guidelines	24
D.2 Additional Discussion on RoBERTa vs. T5	24
D.3 Discussion on the Choice of Regularization Targets	25
D.4 Conceptual Foundations and Synergy of Regularizers	25
D.5 On Applying Representation Learning Principles during Fine-Tuning	26
D.6 Limitations and Future Work	26
D.7 Ethics Statement	26
D.8 Reproducibility	26

A BACKGROUND

A.1 CHALLENGES OF BIAS AND NOISE IN PRE-TRAINING DATA

Bias and noise within pre-training datasets present significant hurdles in constructing dependable machine-learning models. Mislabeled data and imbalanced distributions can lead to models that not only underperform on downstream tasks but also reinforce existing biases (Barocas & Selbst, 2016; Gallegos et al., 2024). This issue is especially problematic in large-scale datasets where

864 manual curation is impractical, and reliance on automated data collection may introduce various
 865 inaccuracies (Northcutt et al., 2021; Birhane & Prabhu, 2021). Consequently, models trained on such
 866 data risk not only poor generalization but also the inheritance of these data-induced flaws, which can
 867 be amplified during adaptation to downstream tasks (Frénay & Verleysen, 2013; Song et al., 2022). A
 868 critical goal of fine-tuning is therefore to learn new capabilities while mitigating the effects of this
 869 "Catastrophic Inheritance".
 870

871 A.2 MITIGATING BIAS THROUGH PARAMETER-EFFICIENT FINE-TUNING

873 Parameter-efficient fine-tuning (PEFT) methods offer a promising foundation for mitigating cata-
 874 strophic inheritance. By design, adapting models with minimal parameter updates can theoretically
 875 limit overfitting to inherited noise and help preserve foundational knowledge (Houlsby et al., 2019;
 876 Zaken et al., 2021; Lester et al., 2021). However, as we argue in the main paper, this promise is not
 877 fully realized in practice. Techniques like low-rank adaptations (LoRA) (Hu et al., 2021) introduce
 878 their own inductive biases, such as the low-rank bottleneck, which can inadvertently exacerbate the
 879 very issues they are meant to solve by amplifying spurious correlations. This critical gap motivates
 880 the development of more principled, explicit regularization techniques—like those proposed in our
 881 work—that are tailored to the unique challenges of the PEFT paradigm.
 882

883 A.3 TYPOLOGIES OF NOISE IN PRE-TRAINING DATA

884 The vast web-scale corpora used to train modern language models, such as LLaMA-2 (Touvron et al.,
 885 2023) and GPT-4 (OpenAI, 2023), inevitably contain significant noise and distributional biases. The
 886 sheer scale of these datasets makes comprehensive manual curation impractical, meaning models are
 887 often exposed to duplicated, corrupted, or irrelevant information during pre-training (Elazar et al.,
 888 2023; Birhane & Prabhu, 2021). When fine-tuned, these models can struggle to distinguish signal
 889 from noise, which in turn degrades downstream performance. Understanding the specific typologies
 890 of this data-induced noise is therefore crucial for developing more robust models. We categorize the
 891 primary challenges as follows.
 892

893 **Low-Quality Data** This category stems from the uncurated nature of web data. A key issue is
 894 **data duplication**, where near-identical content can lead to model overfitting and privacy leakage
 895 risks (Carlini et al., 2022; Hernandez et al., 2022). Another challenge is **data corruption**, where
 896 inconsistent or erroneous inputs degrade model robustness and performance (Fan et al., 2024; Caswell
 897 et al., 2021). Furthermore, **test set contamination**, the leakage of evaluation data into the training
 898 corpus, can lead to inflated performance metrics and invalidate a model's evaluation (Roberts et al.,
 899 2023; Schaeffer, 2023).

900 **Distributional Skew** This form of bias arises from non-uniform data distributions. The most
 901 common form is **category imbalance**, where an underrepresentation of certain topics or classes
 902 causes the model to perform poorly on those categories, leading to biased or unreliable outputs (Xu
 903 et al., 2023; Zhu et al., 2024; Parashar et al., 2024).
 904

905 **Unsafe and Unethical Content** Finally, web corpora often contain undesirable content. The
 906 presence of **toxic and harmful text**, including offensive, biased, or malicious content, can cause the
 907 model to generate inappropriate or harmful outputs, posing significant safety and ethical risks (Zou
 908 et al., 2023; Sun et al., 2024).
 909

910 A.4 EXTENDED RELATED WORK

911 **PEFT and knowledge drift.** Beyond classical PEFT methods such as adapters and LoRA (Houlsby
 912 et al., 2019; Hu et al., 2021), several recent works explicitly study forgetting and knowledge drift
 913 under parameter-efficient adaptation. Smith et al. introduce C-LoRA for continual customization
 914 of text-to-image diffusion models and show that naïve LoRA fine-tuning can cause substantial drift
 915 across tasks, which they mitigate by carefully constraining adapter updates (Smith et al., 2023). Chen
 916 and Garner propose Bayesian parameter-efficient fine-tuning, placing Bayesian priors on LoRA-style
 917 adapters to reduce catastrophic forgetting during continual adaptation (Chen & Garner, 2024). These
 918 approaches share our goal of stabilizing PEFT, but they mainly operate in parameter space and are

evaluated on diffusion or continual-learning settings. In contrast, BA-LoRA targets catastrophic inheritance in language models and uses three output-space regularizers (consistency, diversity, SVD) that are instantiated in a unified way for both NLU and NLG tasks.

Label noise, covariance, and spectral regularization. Our design is also related to work that analyzes and mitigates label noise in large-scale pre-training. Chen et al. propose a feature-space framework that combines consistency, covariance, and dominant-singular-value regularization to improve robustness to noisy labels in pre-training and demonstrate consistent improvements on downstream tasks (Chen et al., 2023; 2025). Their regularizers act on intermediate representations, whereas BA-LoRA applies analogous ideas directly to the output logits of PEFT-adapted models. More broadly, our diversity regularizer is conceptually aligned with redundancy-reduction objectives such as Barlow Twins (Zbontar et al., 2021) and VICReg (Bardes et al., 2021), which encourage high variance and low cross-covariance to avoid representation collapse. BA-LoRA adapts these principles to the supervised, PEFT setting and combines them with an SVD-based spectral smoothing term, yielding a practical recipe for mitigating catastrophic inheritance in both encoder-only and decoder-only language models.

B EXPERIMENTAL SETUP

To rigorously evaluate our proposed method, we conduct a comprehensive set of experiments on a suite of Natural Language Generation (NLG) and Natural Language Understanding (NLU) tasks. Our experimental design, including models, datasets, and training configurations, is detailed below.

B.1 MODELS

Our evaluation leverages a wide array of pre-trained language models to ensure a comprehensive assessment. For NLG tasks, we primarily utilize large language models renowned for their generative capabilities, including LLaMA-2 (7B, 13B) (Touvron et al., 2023), LLaMA-3 (8B, 70B) (AI@Meta, 2024), Mistral-7B-v0.1 (Jiang et al., 2023), Mixtral-8x7B-v0.1 (Jiang et al., 2024), Gemma-7B (Team et al., 2024), Qwen-1.5-7B (Bai et al., 2023), Yi-1.5-34B (Young et al., 2024), and the Mixture-of-Experts model DeepSeek-MoE-16B (Dai et al., 2024).

For NLU tasks, our experiments employ several key models to investigate different aspects of performance. Our main fine-tuning experiments on the GLUE benchmark utilize DeBERTa-v3-base (He et al., 2021). For the controlled study on pre-training data noise, we specifically select RoBERTa-base (Liu et al., 2019) and T5-base (Raffel et al., 2020) due to their distinct corpus characteristics.

A detailed overview of the primary NLU models is presented in Table 6. These models provide a robust foundation for our study due to their diverse pre-training methodologies. For instance, RoBERTa-base was pre-trained on a high-quality mixed corpus, whereas T5-base was pre-trained on the large-scale and noisier C4 web corpus. DeBERTa-v3-base utilized another diverse dataset with a replaced token detection objective. This architectural and methodological diversity is crucial for a thorough evaluation of our approach.

Table 6: Comparison of pre-trained data and methods for various language models.

Model	Pre-trained Data	Pre-training Method
DeBERTa-v3-base (He et al., 2021)	Wikipedia, BooksCorpus, OpenWebText, CC-News, Stories	Replaced Token Detection with GDES
RoBERTa-base (Liu et al., 2019)	BooksCorpus, English Wikipedia, CC-News, OpenWebText, Stories	Masked Language Modeling
T5-base (Raffel et al., 2020)	Colossal Clean Crawled Corpus (C4)	Text-to-Text Denoising Objective

B.2 TASKS, DATASETS, AND METRICS

Natural Language Generation (NLG) For NLG, we assess model capabilities across mathematical reasoning, code generation, and instruction following. The benchmarks include GSM8K (Cobbe et al., 2021), MATH (Yu et al., 2023), HumanEval (Chen et al., 2021), MBPP (Austin et al., 2021), and MT-Bench (Zheng et al., 2024). As summarized in Table 7, evaluation metrics are task-specific: Accuracy for GSM8K and MATH, Pass@1 for HumanEval and MBPP, and GPT-4 based evaluation for MT-Bench.

972
973
974
975
976
977
Table 7: Evaluation metrics for the NLG datasets.
978

Datasets	GSM8K	MATH	HumanEval	MBPP	MT-Bench
Metric	Accuracy	Accuracy	Pass@1	Pass@1	GPT-4 Evaluation

978
979
980
981
982
983
984
Natural Language Understanding (NLU) For our NLU evaluation, we utilized the GLUE benchmark (Wang et al., 2018), which comprises a diverse set of tasks. These tasks can be categorized into three groups: two single-sentence classification tasks (CoLA, SST-2), five pairwise text classification tasks (MNLI, RTE, QQP, MRPC, and QNLI), and one text similarity prediction task (STS-B). Following the standard evaluation protocol, we report Matthew’s correlation for CoLA, Pearson correlation for STS-B, and accuracy for the remaining tasks. For MNLI specifically, we report both matched and mismatched accuracy.

985 986 B.3 IMPLEMENTATION AND TRAINING DETAILS

987
988
989
990
991
992
993
994
Baseline Comparison For a fair and direct comparison, all baseline results presented in our main experiments are directly obtained from their original publications. Specifically, the NLG baseline results in Table 1 are sourced from the comprehensive study by (Yang et al., 2025). For the NLU benchmarks, the results for DeBERTa-v3-base in Table 2 are taken from (Kang & Yin, 2025). For our BA-LoRA runs, we follow the same core fine-tuning configuration (model, dataset splits, optimizer, learning-rate schedule, batch size, and LoRA rank/placements) as in these works, and only introduce our additional regularization terms with coefficients chosen as described in Section 3.1 and Appendix B.4, to ensure a controlled and equitable evaluation.

995
996
997
998
999
For all GLUE experiments, the consistency and diversity regularizers are computed on the fine-tuning data by passing inputs through the pretrained backbone and the BA-LoRA-adapted backbone, using the same shared classification head, to generate teacher and student logits respectively.

1000
1001
1002
1003
1004
1005
1006
1007
1008
1009
1010
1011
MiLoRA vs. BA-LoRA. MiLoRA proposes a spectral variant of LoRA that explicitly exploits *minor* singular components of pretrained weight matrices: instead of parameterizing adapters along the top singular directions (as in PiSSA), MiLoRA allocates capacity to lower-energy directions in weight space, arguing that these under-utilized components can be effective for adaptation while potentially reducing interference with core pretrained knowledge. In contrast, BA-LoRA keeps the underlying LoRA-style parameterization (e.g., standard LoRA, PiSSA, DoRA) and operates entirely in *output space*: it introduces three regularizers on the logits—a consistency term to control knowledge drift, a diversity term to avoid representation collapse, and a spectral SVD term to suppress noisy high-frequency components. Thus, MiLoRA primarily changes *which spectral directions in weight space* are used to represent the adapters, whereas BA-LoRA constrains *how the adapted model behaves* through output-space regularization. These two perspectives are complementary and could, in principle, be combined.

1012
1013
1014
1015
1016
1017
1018
1019
Data Preprocessing for Visualization To analyze the model’s feature space under data imbalance, we constructed a custom imbalanced version of the MNLI training dataset. This process began by separating the full training set into three subsets based on their labels. We then retained all samples from the ‘entailment’ class (100%), while randomly downsampling the ‘neutral’ class to 10% and the ‘contradiction’ class to 1% of their original sizes. Finally, these three subsets were concatenated and shuffled to form the training set for the visualization model, thereby simulating a scenario with a highly skewed label distribution.

1020
1021
1022
1023
1024
1025
t-SNE Visualization For the t-SNE visualization, we fine-tuned a RoBERTa-base model for 3 epochs on the imbalanced MNLI training set described above. Subsequently, we extracted the ‘[CLS]’ token representations from the final hidden layer for all samples in the original, balanced MNLI validation set. These high-dimensional features were projected into two dimensions using the t-SNE algorithm with a perplexity of 30, 1000 iterations, and a fixed random seed (42) for reproducibility. The quality of the resulting clusters was also quantitatively assessed using the silhouette score with a cosine distance metric.

1026 **Evaluation Frameworks** For evaluation, we employed publicly available frameworks. The model’s
 1027 code generation capabilities were assessed using datasets like HumanEval and MBPP through the
 1028 BigCode Evaluation Harness². Instruction-following performance was evaluated using MT-Bench³.
 1029

1030 **B.4 HYPERPARAMETER SETTINGS**
 1031

1032 **NLG (LLaMA-2-7B)** Our Natural Language Generation (NLG) experiments involved fine-tuning
 1033 the LLaMA-2-7B model on a 100,000-sample subset of the MetaMath dataset. The model was
 1034 trained for a single epoch using BFfloat16 (bf16) precision, a maximum sequence length of 512, and
 1035 an effective batch size of 32, achieved with a per-device batch size of 4 and 4 gradient accumulation
 1036 steps. For optimization, we employed the AdamW optimizer with a learning rate of 2×10^{-5} ,
 1037 no weight decay, and a cosine learning rate schedule with a 3% warm-up phase. The base LoRA
 1038 configuration featured a rank (r) of 128, an alpha (α) of 128, and no dropout, with adapters applied
 1039 comprehensively to the ‘q_proj’, ‘k_proj’, ‘v_proj’, ‘o_proj’, ‘gate_proj’, ‘up_proj’, and ‘down_proj’
 1040 layers. For our proposed BA-LoRA method, we set the regularization coefficients to $\lambda_1 = 0.025$,
 1041 $\lambda_2 = 0.005$, and $\lambda_3 = 0.005$. The primary coefficient, λ_1 , also followed a cosine schedule, while the
 1042 lambda focus schedule was set to ‘two_phase’ with a 0.2 warm-up and 0.05 ramp-up ratio. Additional
 1043 parameters for the SVD-based components included an SVD rank (‘svd_k’) of 10, an entropy top-k
 1044 of 20, a distillation temperature of 2.0, and the use of the Frobenius norm for SVD normalization.
 1045

1046 **NLU (GLUE Benchmark)** Our Natural Language Understanding (NLU) experiments on the GLUE
 1047 benchmark involved three models, each with specific hyperparameter configurations as detailed below.
 1048

1049 **DeBERTa-v3-BASE** We fine-tuned DeBERTa-v3-base on the GLUE tasks using the AdamW
 1050 optimizer with a linear learning rate schedule. To strictly align with the PiSSA baseline, we adopted
 1051 a set of task-specific hyperparameters. The LoRA rank (r) was consistently set to 8 across all tasks.
 1052 Other key hyperparameters, including the number of epochs, batch size, learning rate, and LoRA
 1053 alpha, were individually configured for each dataset. The precise configurations are detailed in
 1054 Table 8. **For encoder-only NLU models (e.g., DeBERTa-v3-base on GLUE), we attach a task-specific**
 1055 **linear classification head and compute Z_P and Z_F by passing the same fine-tuning inputs through**
 1056 **the pretrained (teacher) encoder and the BA-LoRA-adapted (student) model, respectively, using the**
 1057 **shared classification head, matching the notation used in Sec. 2.2.1.**

1058 Table 8: Fine-tuning hyperparameters for the DeBERTa-v3-base model on each task of the GLUE
 1059 benchmark. The settings are aligned with the PiSSA baseline.

Dataset	Epochs	Batch Size	Learning Rate	LoRA Alpha
MNLI	5	16	5×10^{-4}	8
SST-2	20	16	3×10^{-5}	8
MRPC	20	32	2×10^{-4}	8
CoLA	20	16	1×10^{-4}	8
QNLI	10	32	1×10^{-4}	16
QQP	10	16	1×10^{-4}	8
RTE	50	16	1×10^{-4}	8
STS-B	20	8	3×10^{-4}	8

1060 **T5-BASE** In our experiments with T5-Base, we fine-tuned all models for a single epoch using FP32
 1061 precision, a maximum sequence length of 128, and a batch size of 32. Optimization was performed
 1062 with the AdamW optimizer (Loshchilov & Hutter, 2019) ($\beta_1 = 0.9$, $\beta_2 = 0.999$, $\epsilon = 1 \times 10^{-8}$, and
 1063 no weight decay), coupled with a learning rate of 1×10^{-4} . The learning rate schedule incorporated
 1064 a 3% warm-up phase followed by a cosine decay. For the LoRA configuration, we set the rank (r) to
 1065 8, alpha (α) to 16, and applied it to all linear modules except for the embedding, layer normalization,
 1066 and language model head layers.
 1067

1068 **RoBERTa-BASE** For fine-tuning RoBERTa-base on the GLUE benchmark, our setup aligns with
 1069 standard practices for LoRA-based methods. We employed the AdamW optimizer with a linear
 1070

1071 ²<https://github.com/bigcode-project/bigcode-evaluation-harness>

1072 ³<https://github.com/lm-sys/FastChat>

learning rate schedule, preceded by a warm-up phase over the first 6% of the total training steps. The LoRA configuration was kept consistent across all tasks: the rank (r) was set to 8 for the query (q) and value (v) projection matrices, and the alpha (α) was set to 8. The maximum sequence length was fixed at 512 tokens. Other crucial hyperparameters, including the number of epochs, batch size, and the peak learning rate, were individually tuned for each GLUE task to ensure optimal performance. The precise per-task configurations are detailed in Table 9.

Table 9: Task-specific hyperparameters for fine-tuning RoBERTa-base with LoRA on the GLUE benchmark.

Hyperparameter	MNLI	SST-2	MRPC	CoLA	QNLI	QQP	RTE	STS-B
Batch Size	16	16	16	32	32	16	32	16
# Epochs	30	60	30	80	25	25	80	40
Learning Rate	5×10^{-4}	5×10^{-4}	4×10^{-4}	4×10^{-4}	4×10^{-4}	5×10^{-4}	4×10^{-4}	4×10^{-4}

C MORE EXPERIMENTS

Table 10: Impact of the proposed regularization framework on various LoRA-style methods, evaluated on LLaMA-2-7B. "Reg" denotes the application of our three regularization terms. All results are averaged over 3 runs.

Method	GSM8K	MATH	HumanEval	MBPP	MT-Bench	Avg
LoRA	42.68 ± 0.54	5.92 ± 0.15	16.80 ± 0.38	21.51 ± 0.43	4.60 ± 0.14	18.30
LoRA + Reg	51.82 ± 0.36	8.69 ± 0.39	21.03 ± 0.58	33.81 ± 0.51	4.73 ± 0.24	24.02
DoRA	41.77 ± 0.74	6.20 ± 0.48	16.86 ± 0.54	21.60 ± 0.49	4.48 ± 0.14	18.18
DORA + Reg	52.71 ± 0.42	8.23 ± 0.27	21.05 ± 0.31	34.78 ± 0.28	4.96 ± 0.22	24.35
PiSSA	51.48 ± 0.34	7.60 ± 0.18	19.48 ± 0.45	23.84 ± 0.46	4.92 ± 0.07	21.46
BA-LoRA (PiSSA + Reg)	55.86 ± 0.35	9.47 ± 0.52	23.58 ± 0.25	36.86 ± 0.31	5.11 ± 0.05	25.90

C.1 GENERALITY OF THE REGULARIZATION FRAMEWORK

To verify that our regularization framework's benefits extend beyond PiSSA, we integrated it with standard LoRA and DoRA. The results, presented in Table 10, demonstrate the framework's broad applicability and yield a crucial insight. While our regularizers provide substantial performance gains across all tested methods, their effect on standard LoRA is particularly noteworthy. Augmenting standard LoRA with our regularizers is sufficient to match and even surpass the performance of the more advanced PiSSA baseline. This finding underscores that our regularization framework can function as a powerful, model-agnostic enhancement for a wide range of PEFT methods.

Despite the strong standalone performance of the regularizers, the optimal results are consistently achieved by our full BA-LoRA model. This indicates that PiSSA's principled initialization provides a superior foundation upon which our regularization framework can build, leading to the highest overall performance. This validates our integrated approach as the most effective configuration for mitigating catastrophic inheritance and achieving state-of-the-art results.

C.2 HYPERPARAMETER SENSITIVITY ANALYSIS

To validate the principled selection of our framework's hyperparameters, we conducted a detailed sensitivity analysis. Centered around our final BA-LoRA configuration on LLaMA-2-7B, this study systematically investigates the influence of the core regularization coefficients ($\lambda_1, \lambda_2, \lambda_3$) by perturbing them from their default values. The results, visualized in Figure 4, reveal a broad region of stable performance, supporting the robustness of our chosen configuration.

Sensitivity to the Consistency Anchor (λ_1) As illustrated in Figures 4(a,b), we vary λ_1 across $\{0.0125, 0.025, 0.0375\}$ while keeping $\lambda_2 = \lambda_3 = 0.005$. Performance on both MATH and GSM8K remains highly stable across this range, with only minor fluctuations, indicating a broad region of insensitivity. Our chosen value of $\lambda_1 = 0.025$, highlighted as the optimal point in the figure, is

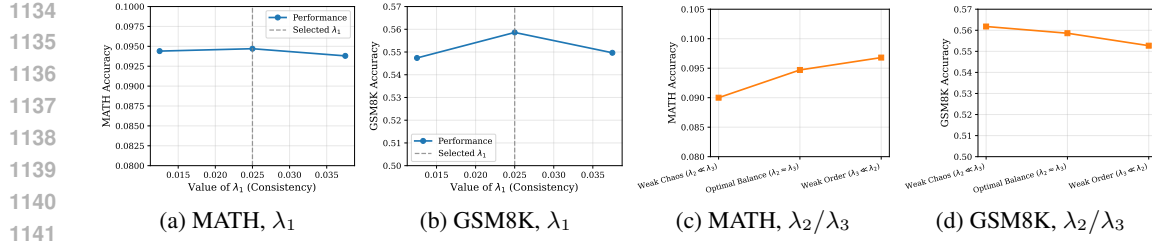


Figure 4: Sensitivity analysis of the core BA-LoRA regularization coefficients. Panels (a,b) show the effect of varying the consistency weight λ_1 on MATH and GSM8K separately, and panels (c,d) show the effect of changing the balance between λ_2 and λ_3 .

thus empirically validated as a robust setting that balances preserving pre-trained knowledge with acquiring new task-specific capabilities.

Sensitivity to the Symbiotic Balance (λ_2 and λ_3) Next, we investigate the symbiotic balance between the other two regularizers, which govern a trade-off between performance on the two reasoning benchmarks (MATH and GSM8K). As shown in Figures 4(c,d), we compare our final configuration’s balanced setting ($\lambda_2 \approx \lambda_3$) against two asymmetric conditions: a “Weak Chaos” setting ($\lambda_2 \ll \lambda_3$), where the structural regularizer (λ_3) dominates, and a “Weak Order” setting ($\lambda_3 \ll \lambda_2$), where the diversity regularizer (λ_2) is dominant. The results reveal a clear trade-off: disrupting the equilibrium leads to specialized improvements on one benchmark at the cost of the other, while the balanced configuration provides strong performance on both.

C.3 ANALYSIS ACROSS DIVERSE MODEL ARCHITECTURES AND SCALES

To assess the generalizability and robustness of BA-LoRA, we conducted a comparison against LoRA and PiSSA across ten distinct pre-trained models. This set includes models of varying scales (e.g., LLaMA-2-7B up to LLaMA-3-70B) and architectures, featuring both standard dense models and Mixture-of-Experts (MoE) models such as Mixtral-8x7B. All methods were fine-tuned on a blend of reasoning and code datasets (MetaMathQA-100K and CodeFeedback-100K) and evaluated on GSM8K and HumanEval.

As visualized in Figure 5, BA-LoRA typically achieves the best or near-best performance among LoRA-style methods on both benchmarks, across most model families and scales. The gains over LoRA and PiSSA are especially pronounced on several mid- and large-scale models, suggesting that our regularization framework remains effective beyond the LLaMA-2-7B setting.

Furthermore, this performance advantage largely carries over to computation-constrained settings. The figure also plots the performance of 4-bit quantized versions of each method (QLoRA, QPiSSA, and QBA-LoRA). The overall trend is similar: QBA-LoRA generally matches or exceeds the other quantized baselines, indicating that the benefits of our framework are robust to quantization and remain useful for resource-efficient deployment.

C.4 PERFORMANCE ANALYSIS ACROSS DIFFERENT RANKS

We analyzed the performance of BA-LoRA, PiSSA, and LoRA across a range of ranks (from 1 to 128) on the LLaMA-2-7B and Mistral-7B-v0.1 models. Each method was fine-tuned for one epoch on the MetaMathQA-100K dataset and evaluated on GSM8K and MATH. The results, presented in Figure 6, show that BA-LoRA consistently outperforms both LoRA and PiSSA across all ranks, models, and tasks, demonstrating its stable and universal superiority. Furthermore, both BA-LoRA and PiSSA exhibit the remarkable ability to surpass the performance of full fine-tuning at higher ranks, with BA-LoRA often achieving this milestone at relatively low ranks (e.g., rank 16-32). This highlights the strong regularization effect of our approach, as standard LoRA consistently lags behind the full fine-tuning baseline. Moreover, the performance advantage of BA-LoRA over its counterparts is even more pronounced on the Mistral-7B-v0.1 model, suggesting its benefits generalize effectively across different foundational model architectures. These results collectively validate BA-LoRA as a highly efficient and superior fine-tuning method.

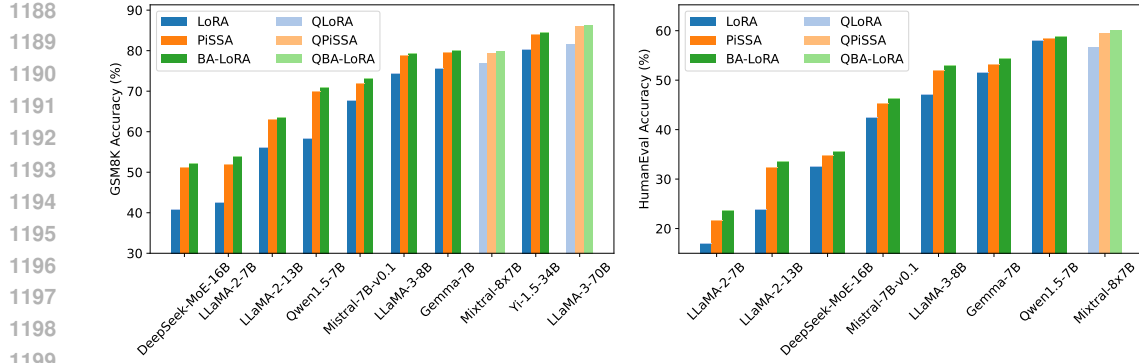


Figure 5: Performance comparison of different models on the GSM8K and HumanEval benchmarks.



Figure 6: Performance comparison of full fine-tuning, LoRA, PiSSA, and BA-LoRA across different ranks.

C.5 COMPARISON OF REGULARIZATION OBJECTIVES FOR NLU

To empirically validate our design choice of Covariance Regularization ($\mathcal{L}_{DR,NLU}$) over Entropy Regularization (commonly used in NLG) for discriminative tasks, we conducted a comparative study on the MNLI benchmark. While entropy minimization is effective for generation, we hypothesized that applying it sample-wise to noisy or imbalanced NLU data may inadvertently encourage the model to be “confidently wrong” on minority classes, rather than effectively preventing representation collapse. The results presented in Table 11 support this hypothesis. Notably, substituting our covariance-based regularizer with an entropy-based one results in performance (90.41%) that is not only inferior to our method (91.26%) but also falls below the standard LoRA baseline (90.71%). This finding confirms that batch-wise feature decorrelation is a structurally superior strategy for mitigating representation collapse in discriminative fine-tuning.

Table 11: Comparison of diversity regularization objectives on MNLI (DeBERTa-v3-base).

Method	MNLI Accuracy
Standard LoRA	90.71
BA-LoRA (w/ Entropy Reg.)	90.41
BA-LoRA (w/ Covariance Reg.)	91.26

C.6 QUANTITATIVE ANALYSIS OF CLUSTER QUALITY AND MINORITY REPRESENTATION

To complement the visual analysis provided in Figure 3 (main text), we conduct a quantitative evaluation of the feature space separation under the imbalanced fine-tuning setting (MNLI task). We compute metrics in the original high-dimensional logit space (before t-SNE projection) to avoid dimensionality reduction artifacts. We report the **Global Silhouette Score** (over all classes), the **Minority-Class Silhouette Score** (measuring the isolation of the minority cluster), and the **Minority-Class Recall** (measuring classification accuracy on the minority class).

Table 12 presents the results. Standard LoRA exhibits a near-zero minority silhouette score (0.015) and a trivial minority recall (5.8), quantitatively confirming the representation collapse observed visually. In contrast, BA-LoRA achieves a significantly higher minority silhouette score (0.425) and restores the minority recall to 61.7. These results demonstrate that BA-LoRA effectively mitigates the catastrophic inheritance of pre-trained priors, enabling the model to establish a distinct and semantically meaningful decision boundary for the minority class.

Table 12: Quantitative analysis of feature separation and classification performance on the minority class (MNLI imbalanced setting). Metrics are computed in the high-dimensional logit space.

Method	Global Silhouette (All Classes)	Minority-Class Silhouette (Cluster Quality)	Minority-Class Recall (Accuracy (%))
Standard LoRA	0.207	0.015	5.8
PiSSA	0.247	0.128	26.4
BA-LoRA (Ours)	0.351	0.425	61.7

D MORE DISCUSSIONS

Here, we offer further insights into our work.

D.1 PRACTICAL HYPERPARAMETER GUIDELINES

For a new model–task configuration, BA-LoRA can be tuned with a simple recipe, without fragile fine-grained search. First, choose initial values for $\lambda_{\text{consistency}}$, $\lambda_{\text{diversity}}$, and λ_{svd} such that, on a small calibration batch, each regularization term contributes a **meaningful fraction to the total loss (ensuring gradient magnitudes are commensurate with the task loss)**, so that no component is inactive or overwhelmingly dominant. Second, keep the ratios between the three coefficients fixed and tune a single global scale λ_{global} that multiplies all of them, i.e., $\lambda_i \leftarrow \lambda_{\text{global}} \lambda_i$ for $i \in \{\text{consistency, diversity, svd}\}$; in our experience, a coarse search over a few values (e.g., $\{0.5, 1.0, 2.0\}$) on a held-out validation split is sufficient. Third, if needed, individual coefficients can be adjusted by coarse factors (such as $\times 0.5$ or $\times 2$) to emphasize preserving pretrained knowledge (larger $\lambda_{\text{consistency}}$), avoiding collapse (larger $\lambda_{\text{diversity}}$), or suppressing noisy high-frequency components (larger λ_{svd}).

As shown by the ablation study in Section 3.2.4 and the sensitivity analysis in Appendix C.2, BA-LoRA achieves stable performance around these configurations and consistently outperforms vanilla LoRA and PiSSA in this region, suggesting that this lightweight procedure is sufficient in practice. Moreover, for each backbone we fix a single configuration of the auxiliary hyperparameters (s, T, K, k) based on a small validation experiment and reuse it across all datasets, avoiding per-benchmark tuning. **Given the stability observed in our preliminary experiments, and to maintain efficiency**, we use these as reasonable per-backbone defaults rather than performing an exhaustive, computationally expensive sensitivity sweep.

D.2 ADDITIONAL DISCUSSION ON ROBERTA vs. T5

Section 3.2.2 uses RoBERTa-base and T5-base as a natural comparison for probing robustness to inherited noise, since RoBERTa is trained on a curated mixture of corpora while T5 is pretrained primarily on the C4 web corpus. However, these models also differ in architecture (encoder-only vs. encoder–decoder) and pre-training objective (masked LM vs. text-to-text denoising). As a result, the larger BA-LoRA gains we observe on T5 should be interpreted as evidence that is compatible with our noisy-pretraining hypothesis, rather than a fully controlled causal test. A more definitive analysis would require models with closely matched architectures and objectives but systematically varied pre-training corpora, which we leave for future work.

1296 D.3 DISCUSSION ON THE CHOICE OF REGULARIZATION TARGETS
12971298 A key design choice in BA-LoRA is the application of regularization terms in the model’s output
1299 space (i.e., on logits and their derived distributions) rather than directly on the trainable adapter
1300 parameters (A and B). This section provides further justification for this principled decision.
13011302 Regularizing the low-rank adapter weights directly, for instance, by penalizing the norm of A or B ,
1303 is a viable alternative. However, this approach presents a significant challenge: the mapping from
1304 the low-dimensional parameter space of the adapters to the high-dimensional functional space of
1305 the model’s final output is highly complex and non-linear. Consequently, a simple constraint on
1306 the adapter weights (e.g., a small norm) does not guarantee the desired functional behavior (e.g.,
1307 output diversity or consistency with the pre-trained model). The effect of such parameter-space
1308 regularization on the final model output is often unpredictable and difficult to control.
13091310 In contrast, applying regularization directly in the output space offers a more direct and interpretable
1311 path to achieving our goals. By directly penalizing undesirable properties in the output logits or
1312 probability distributions—such as their deviation from the pre-trained model (Knowledge Drift), their
1313 lack of diversity (Representation Collapse), or their over-reliance on non-robust features (Overfitting
1314 to Noise)—we are explicitly constraining the model’s final behavior. This approach ensures that
1315 our optimization objective is perfectly aligned with the ultimate goal of mitigating the functional
1316 consequences of Catastrophic Inheritance. The strong and consistent performance of our framework
1317 across diverse models, tasks, and ranks, as demonstrated in our experiments, serves as powerful
1318 empirical validation for this output-space regularization strategy.
13191320 D.4 CONCEPTUAL FOUNDATIONS AND SYNERGY OF REGULARIZERS
13211322 The three regularization terms proposed in BA-LoRA—consistency, diversity, and SVD-based
1323 regularization—were not chosen arbitrarily. Each is inspired by well-established principles in the
1324 machine learning literature for improving model robustness and generalization, and they are designed
1325 to work in synergy.
13261327 **Origins.** The **Consistency Regularizer** (implemented as a [KLD-based distillation loss in our experiments](#)) is a form of knowledge distillation (Hinton et al., 2015), specifically self-distillation,
1328 where the pre-trained model acts as the teacher. The **Diversity Regularizer** is rooted in principles
1329 from representation learning and information theory. The covariance-based term for NLU is directly
1330 inspired by methods that combat representation collapse in self-supervised learning (Bardes et al.,
1331 2021), while the entropy-based term for NLG is a classic technique to prevent mode collapse and
1332 improve diversity in generative models (Cover, 1999). Finally, the **SVD Regularizer** builds upon
1333 the principle of spectral regularization, where the singular value spectrum of a weight or feature
1334 matrix is constrained to improve generalization. The insight that dominant singular values capture the
1335 most robust data patterns is a recurring theme in robust machine learning and transfer learning (Chen
1336 et al., 2019). [Throughout our experiments we follow the standard temperature-scaled distillation convention](#) (Hinton et al., 2015) and multiply the KL-based distillation loss by T^2 . Since dividing
1337 logits by T scales the gradients of the KL divergence approximately as $1/T^2$, this factor keeps the
1338 effective gradient norm of the consistency loss roughly invariant to T , so that changing T primarily
1339 controls the softness of the teacher distribution rather than unintentionally reweighting the regularizer.
13401341 **Synergy.** While each regularizer addresses a distinct failure mode, their combination creates a
1342 synergistic effect. For instance, solely enforcing consistency (\mathcal{L}_{CR}) might excessively constrain the
1343 model, preventing it from fully adapting to the downstream task. However, when combined with the
1344 diversity regularizer (\mathcal{L}_{DR}), the model is encouraged to explore new, diverse representations within
1345 the bounds of the pre-trained knowledge. Similarly, the SVD regularizer ($\mathcal{L}_{\text{SVDR}}$) helps ensure that
1346 the diverse representations learned are also the most robust and generalizable ones, preventing the
1347 model from learning spurious correlations encouraged by a simple diversity objective. Our ablation
1348 study (Section 3.2.4) empirically confirms this synergy, showing that the performance of the full
1349 BA-LoRA model surpasses the sum of the individual components’ contributions.

1350
1351

D.5 ON APPLYING REPRESENTATION LEARNING PRINCIPLES DURING FINE-TUNING

1352
1353
1354
1355

A key consideration for our work is whether incorporating principles from self-supervised learning (SSL), such as our diversity regularizer, during fine-tuning could disrupt the model’s pre-trained representations. We contend that our framework effectively mitigates this risk through two primary mechanisms.

1356
1357
1358
1359

First, the PEFT paradigm, specifically LoRA, inherently limits the scope of any changes. With the vast majority of parameters frozen, the model’s core representational geometry remains anchored. Our regularizers guide only the small perturbations introduced by the low-rank adapters, ensuring these updates refine rather than overwrite the foundational knowledge.

1360
1361
1362
1363
1364
1365
1366

Second, our regularization scheme is synergistic. The consistency regularizer (\mathcal{L}_{CR}) acts as a crucial counterweight to the diversity regularizer (\mathcal{L}_{DR}). While \mathcal{L}_{DR} encourages adaptation and prevents representation collapse on the downstream task, \mathcal{L}_{CR} ensures this adaptation does not stray from the pre-trained model’s robust knowledge manifold. It is precisely this calibrated balance—what we term “guided exploration within a trusted neighborhood”—that allows BA-LoRA to enhance task-specific performance without inducing catastrophic forgetting.

1367
1368

D.6 LIMITATIONS AND FUTURE WORK

1369
1370
1371
1372
1373
1374
1375
1376
1377
1378
1379

While this study validates the effectiveness of BA-LoRA, there are areas for future research. Our empirical evaluation has primarily focused on English-language benchmarks, which are a robust foundation for BA-LoRA; however, future work should extend this validation to multilingual settings and specialized domains to ensure broader applicability of the method. **Moreover, our analysis of noisy pre-training in Sec. 3.2.2 relies on RoBERTa-base and T5-base checkpoints, which differ in both architecture and pre-training objective; results should be interpreted as suggestive rather than controlled evidence about pre-training noise, and a more definitive study with a fixed architecture pre-trained under systematically varied noise levels is an important direction for future work.** In addition, while BA-LoRA’s regularization components have shown strong promise, task-specific adaptations could further optimize their performance across a wider range of applications, and exploring such adjustments will be valuable for enhancing robustness and adaptability in diverse use cases.

1380
1381

D.7 ETHICS STATEMENT

1382
1383
1384
1385
1386
1387
1388
1389
1390
1391

This study aims to develop and evaluate BA-LoRA, a novel parameter-efficient fine-tuning method designed to mitigate bias and enhance the performance of LLMs. By aiming to create more robust and less biased models, a primary ethical motivation of this work is to contribute to safer and more reliable AI systems. Our research utilizes existing open-source public datasets for both fine-tuning and evaluation purposes. For Natural Language Generation tasks, we employed widely recognized datasets within the research community, including MetaMathQA, CodeFeedback, and WizardLM-Evol-Instruct. These datasets have no known ethical concerns. For Natural Language Understanding tasks, we utilized the GLUE benchmark, standard evaluation dataset in machine learning. We are committed to the responsible development and application of AI technologies. Throughout this research, we will continue to monitor and address any ethical issues that may arise.

1392
1393

D.8 REPRODUCIBILITY

1394
1395
1396
1397
1398
1399
1400

To ensure the reproducibility of our results, we provide a detailed description of our experimental setup in Section 3.1 and Appendix Section B, including model introduction, dataset introduction, hyperparameter configuration, and evaluation procedures. All models and datasets used are publicly available. In addition, we have refined the implementation scripts and fine-tuning strategies to facilitate independent verification. To further facilitate reproducibility, our source code, including scripts to replicate all main experiments, will be made publicly available upon acceptance.

1401
1402
1403

USE OF LARGE LANGUAGE MODELS

In the preparation of this manuscript, a large language model (LLM) was utilized as a writing assistant. The LLM’s role was strictly limited to improving the clarity, conciseness, and grammatical

1404 correctness of the text. Specifically, it was used for tasks such as rephrasing sentences, suggesting
1405 alternative vocabulary, and checking for stylistic consistency. All core scientific ideas, experimental
1406 designs, data analyses, and final conclusions were conceived and formulated exclusively by the
1407 human authors.

1408

1409

1410

1411

1412

1413

1414

1415

1416

1417

1418

1419

1420

1421

1422

1423

1424

1425

1426

1427

1428

1429

1430

1431

1432

1433

1434

1435

1436

1437

1438

1439

1440

1441

1442

1443

1444

1445

1446

1447

1448

1449

1450

1451

1452

1453

1454

1455

1456

1457